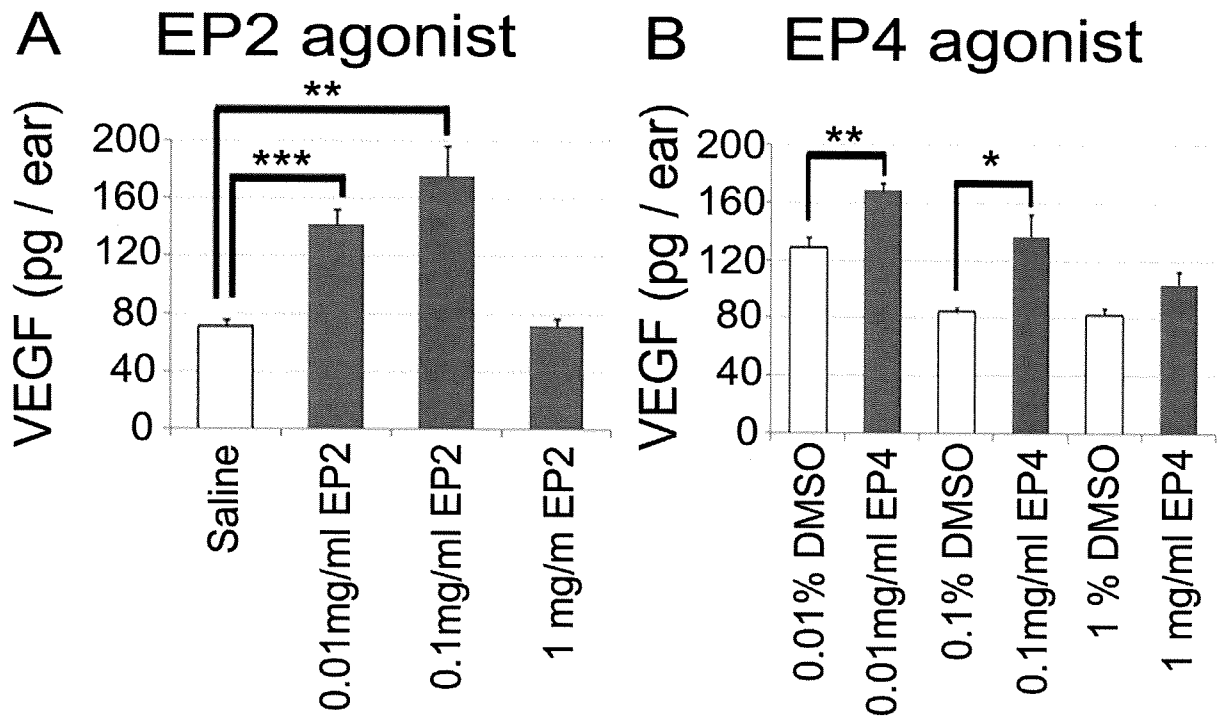

Figure 2 VEGF protein levels in the inner ear measured by ELISA. (A) VEGF protein levels in samples treated with 0.01 or 0.1 mg/ml EP2 agonist were significantly higher than those in samples treated with physiological saline (**, $p < 0.01$, and ***, $p < 0.001$, ANOVA with Scheffe's method). (B) VEGF protein levels in samples treated with 0.01 or 0.1 mg/ml EP4 agonist were significantly higher than those in samples treated with 0.01 or 0.1% DMSO, respectively (*, $p < 0.05$, **, $p < 0.01$, Student's *t*-test).

ganglion neurons in response to an EP2 or EP4 agonist acts on cells expressing Flt-1 and/or Flk-1 in the cochlea in a paracrine or autocrine fashion.

Discussion

Recently, the prostaglandin E receptor subtypes EP1, EP2, EP3 and EP4 were cloned, and their specific agonists were purified [7]. EP2 and EP4 are coupled to G-protein stimulation and mediate increases in cAMP, while the activation of EP3 leads to a decrease of cAMP levels. We thus hypothesized that selective agonists for EP2 and EP4 might be more effective than PGE1 for the treatment of SNHL. In a previous study, we demonstrated the expression of EP4 in the cochlea, and the attenuation of noise-induced damage as a result of local EP4 agonist administration [9]. However, the mechanisms underlying the protective effect of EP4 against on cochlear damage have not previously been investigated. In the present study, we highlighted VEGF induction via EP2 or EP4 activation. The present study therefore examined the effects of EP2 and EP4 agonists on the modulation of inner ear VEGF levels.

We initially confirmed that EP2 expression occurred in the cochlea and showed a similar pattern to EP4 expression [9]. ELISA and real-time qRT-PCR analyses demonstrated an increase of VEGF protein and mRNA levels in the inner ear after local EP2 or EP4 agonist application, indicating that the stimulation of EP2 and/or EP4 activates VEGF production in the inner ear. Immunostaining for VEGF showed that the strongest response to EP2 or EP4 stimulation occurred in the spiral ganglion neurons, suggesting that they are responsible for increasing the VEGF levels in the inner ear. In addition, expression of the VEGFRs Flt-1 and Flk-1 was identified in the sensory epithelial cells, spiral ganglion neurons, spiral ligament fibrocytes, and stria vascularis marginal cells, which was consistent with previous findings [21]. These results indicate that EP2 and EP4 are involved in the mechanisms underlying the autocrine and paracrine functions of VEGF in the inner ear. For mechanisms of VEGF induction via EP2 or EP4 activation, recent studies have indicated involvement of cAMP- and PKA-dependent mechanisms via SP-1 transcription factor binding sites on the VEGF promoter [12,24,25]. However, further studies are needed to determine signaling cascades for VEGF induction via EP2 and EP4 in the inner ear.

VEGF was initially identified as a mitogen for endothelial cells, which promotes angiogenesis and vascular permeability. Numerous studies have demonstrated that VEGF plays crucial roles in the development and protection of neuronal cells [17,26]. VEGF and its receptors are also present in the cochlea, and have been shown to play

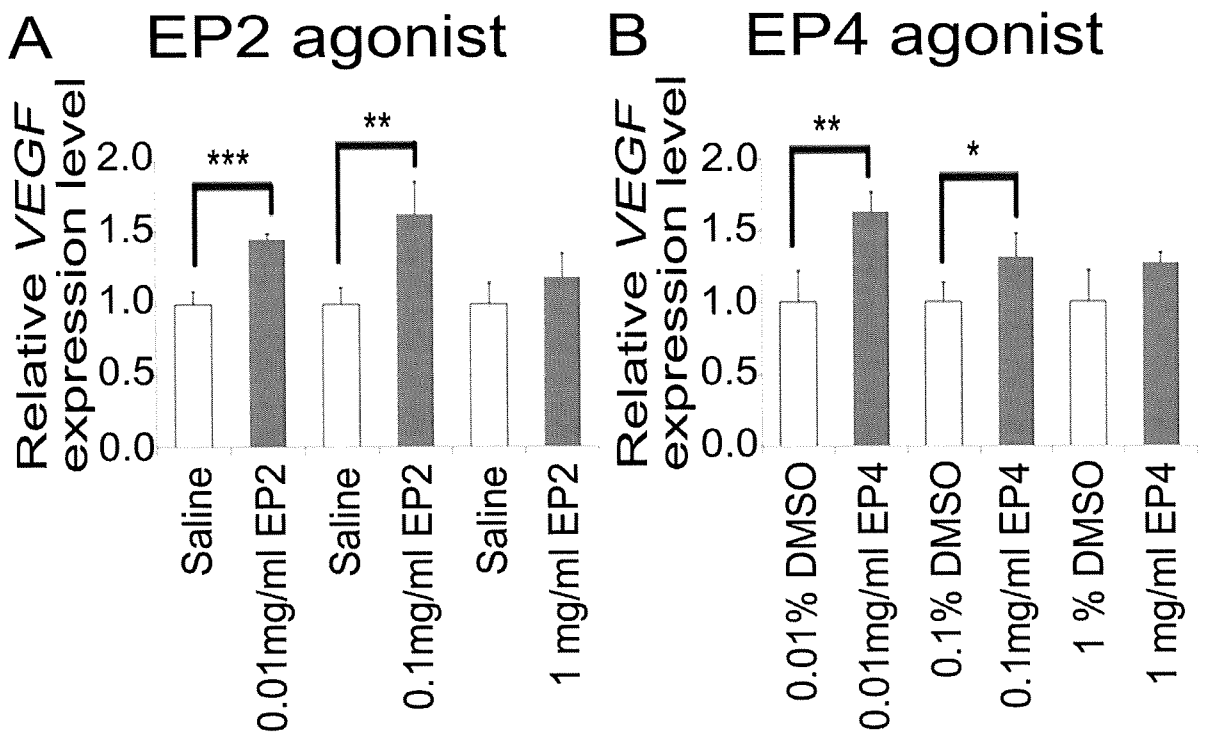

Figure 3 Relative *VEGF* expression levels in inner ear according to real-time qRT-PCR. (A) Samples treated with EP2 agonist at 0.01 or 0.1 mg/ml expressed higher levels of *VEGF* mRNAs than those treated with physiological saline. (B) Samples treated with EP4 agonist at 0.01 or 0.1 mg/ml expressed higher levels of *VEGF* mRNAs than those treated with 0.01 or 0.1% DMSO, respectively (*, $p < 0.05$, **, $p < 0.01$, and ***, $p < 0.001$, Student's *t*-test).

significant roles in the maintenance of cochlear homeostasis [20,21,27-30]. The present findings provide new insights into the mechanisms underlying the regulation of VEGF expression in the cochlea, which is mediated by EP2 and EP4. Past work has demonstrated that hypoxia-inducible factor-1 induces VEGF upregulation in the cochlea, which is involved in the cochlear pericyte responses to noise trauma [30]. In the central nervous system, VEGF synthesized by neurons was reported to promote survival and angiogenesis, as well as autocrine and paracrine neuronal survival [31]. The present results demonstrated spiral ganglion neuron responses to EP2 and EP4 stimulation, and the expression of both Flt-1 and Flk-1 in various cochlear components including the sensory epithelium, spiral ganglion, and stria vascularis. Flk-1 appears to mediate almost all of the known cellular responses to VEGF [32], suggesting that Flk-1 also plays an essential role in VEGF function in the cochlea. However, an actual answer for this awaits further investigations. Consequently, present findings indicate that VEGF has autocrine and paracrine effects on neuronal and endothelial cells in the cochlea as well as in the central nervous system, and that EP2 and EP4 are involved in

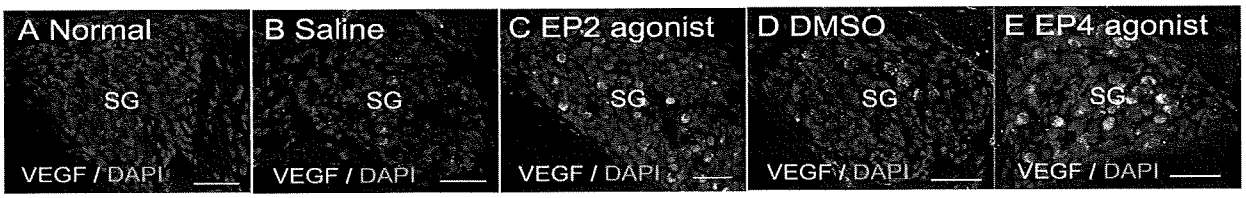

Figure 4 Immunoreactivity for VEGF in the spiral ganglion cells. Little or no staining was detected in the spiral ganglion cells of the untreated samples (A; Normal). VEGF expression (green) was weakly detected in a few spiral ganglion neurons in samples treated with physiological saline (B; Saline) and those treated with 0.1% DMSO (D; DMSO). VEGF expression was strongly detected in a large number of the spiral ganglion neurons treated with EP2 agonist (C; EP2 agonist) or EP4 agonist (E; EP4 agonist). Nuclei were labeled with DAPI. The specimens were viewed with 63× oil objective. Scale bar = 200 μm.

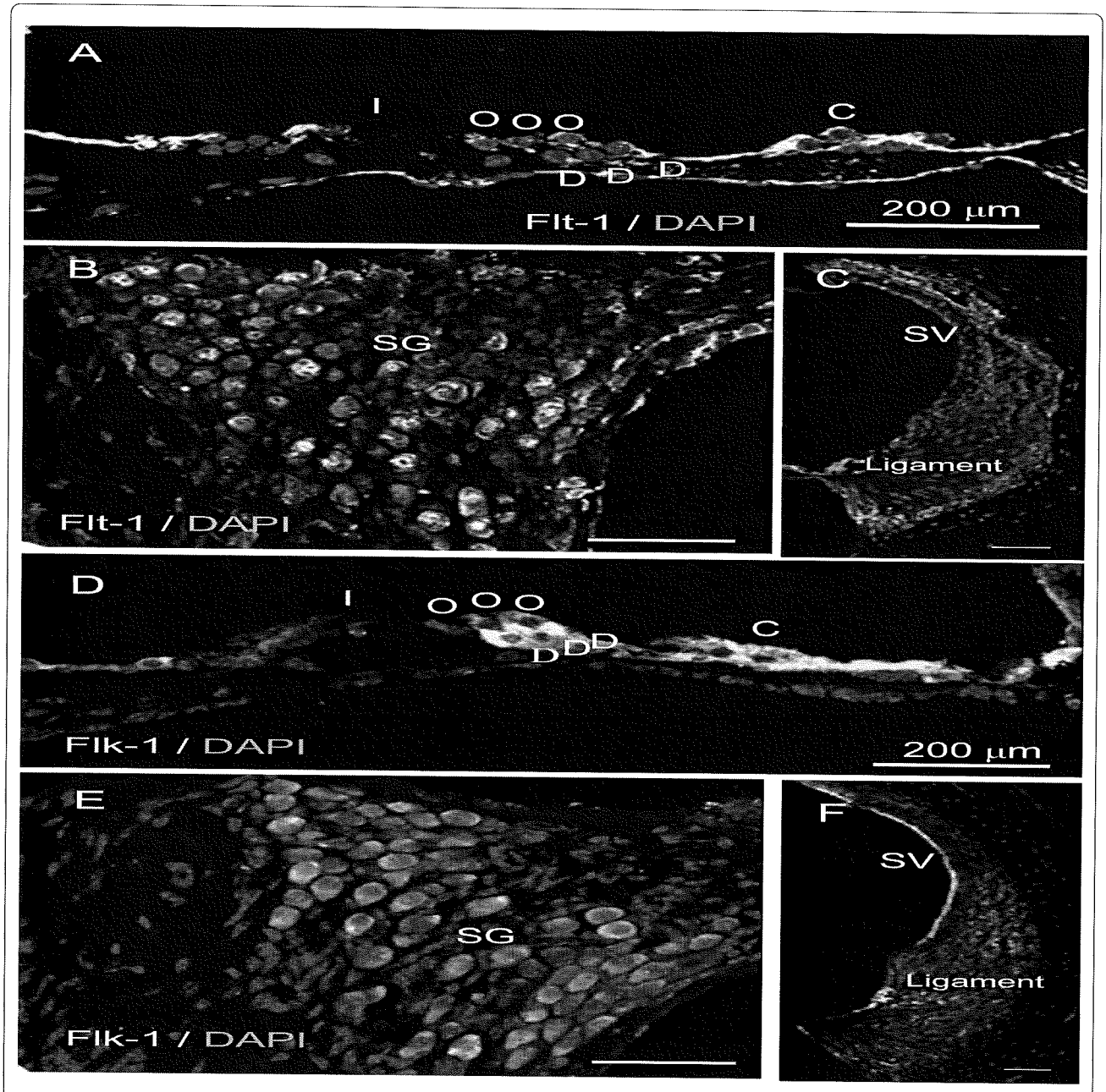

Figure 5 Immunoreactivity for Flt-1 and Flk-1 in the cochlea. (A-C) Flt-1 expression (green) was detected n the cochlear sensory epithelium (A; I, inner hair cell; O, outer hair cell; D, Deiter's cell; C, Claudius' cell), spiral ganglion neurons (B; SG) and spiral ligament (C; ligament). (D-F) Flk-1 expression was found in the cochlear sensory epithelium (D), spiral ganglion neurons (E), spiral ligament (F) and stria vascularis (F; SV). Nuclei were labeled with DAPI. The specimens were viewed with 63× oil objective. Scale bar = 200 μm.

autocrine and paracrine functions of VEGF in the cochlea.

Hypoxic preconditioning is known to have protective effects on neurons [33,34]. Recently, VEGF was reported to be involved in the protective effect of neuronal preconditioning against ischemic injury [35]. Protection against noise exposure by cochlear preconditioning has also been documented [36]. VEGF upregulation in the cochlea is induced not only by intense noise exposure [20,30] but also by moderate noise exposure [21]. These findings suggest that VEGF is also involved in the mechanisms underlying protection against noise exposure by cochlear preconditioning. Our previous study demonstrated that pretreatment with an EP4 agonist led to almost complete protection of the cochleae against noise trauma [9]. In addition, our present findings demonstrate the involvement of EP2 and EP4 in the regulation of VEGF synthesis in the inner ear. EP2-mediated and EP4-mediated VEGF

synthesis in the cochlea could therefore be associated with protection against noise by cochlear preconditioning. However, distinct roles of VEGF in cochlear protection by local application of EP2 or EP4 agonists have not been elucidated. Further studies are required to determine whether VEGF antagonists suppress protective effects of EP2 or EP4 agonists for cochleae.

Conclusions

The present study demonstrated that local EP2 and EP4 agonist treatment induces VEGF synthesis in the inner ear, especially in the spiral ganglion neurons. The expression of VEGFRs was detected in the cochlear sensory epithelium, spiral ganglion, spiral ligament, and stria vascularis. These findings indicate the involvement of EP2 and EP4 in the autocrine and paracrine functions of VEGF in the cochlea.

Methods

Animals

Male C57BL/6 mice at 8 weeks of age were purchased from Japan SLC, Inc. (Hamamatsu, Japan). The Animal Research Committee of the Graduate School of Medicine, Kyoto University, Japan, approved all of the experimental protocols. Animal care was supervised by the Institute of Laboratory Animals of the Graduate School of Medicine, Kyoto University. All of the experimental procedures were performed in accordance with the National Institutes of Health (NIH) Guide for the Care and Use of Laboratory Animals.

EP2 expression in cochleae

The expression of EP2 in the cochlea was immunohistochemically examined using normal cochlear specimens (n = 3). Under general anesthesia with midazolam (10 mg/kg; Astellas, Tokyo, Japan) and xylazine (10 mg/kg; Bayer, Tokyo, Japan), the animals were transcardially perfused with 0.01 M phosphate-buffered saline (PBS; pH 7.4) followed by 4% paraformaldehyde (PFA) in PBS. The temporal bones were immediately dissected out and immersed in the same fixative for 2 h at 4°C. After decalcification with 0.1 M ethylenediamine tetra-acetic acid (EDTA) for 7 days at 4°C, 10-μm-thick cryostat sections were prepared. Two midmodiolus sections from each cochlea were subjected to immunostaining for EP2. Anti-EP2 polyclonal antibody (dilution, 1:250; Cayman Chemical, Ann Arbor, MI, USA) was used as the primary antibody, and Alexa 568-conjugated goat anti-rabbit immunoglobulin G (IgG; dilution, 1:500; Invitrogen, Carlsbad, CA, USA) was used as the secondary antibody. After immunostaining for EP2, the nuclei were counterstained with 4,6-diamidino,2-phenylindole dihydrochloride (DAPI; 1 μg/ml in PBS; Molecular Probes, Eugene, OR, USA). Heart specimens obtained from the mice were used as positive controls for EP2. Nonspecific labeling was tested by blocking protein-antibody complex formation using EP2-blocking peptide (Cayman Chemical). The specimens were viewed with a Leica TCS-SPE confocal microscope (Leica Microsystems, Wetzlar, Germany).

Local application of EP2 or EP4 agonist to inner ears

The EP2 agonist ONO-AE1-259-01 and the EP4 agonist ONO-AE1-329 (both from Ono Pharmaceutical Co., Ltd., Osaka, Japan) were used in this study. The EP2 agonist was dissolved in physiological saline to give a final concentration of 0.01, 0.1, or 1 mg/ml. The EP4 agonist was dissolved in DMSO and diluted with physiological saline to give a final concentration of 0.01, 0.1, or 1 mg/ml containing 0.01, 0.1, or 1% DMSO, respectively. Controls for EP2 agonist application were treated with saline, and controls for EP4 agonist application were treated with 0.01, 0.1, or 1% DMSO. Drug application was performed under general anesthesia with midazolam and xylazine as previously reported [37-39]. A retroauricular incision was made in the left ear, and the posterior semicircular canal (PSCC) was exposed. A small hole was made in the bony wall of the PSCC. A fused silica glass needle (EiCOM, Kyoto, Japan) was then inserted into the perilymphatic space of the PSCC, and the appropriate material was injected at a rate of 0.5 μl/min for 4 min (total = 2 μl) using a micro syringe pump (EiCOM). At 24 h after the injection into the PSCC, the animals were transcardially perfused with PBS under general anesthesia with midazolam and xylazine, and the inner ears were immediately dissected out. The inner ear samples were subjected to ELISA or real-time qRT-PCR analysis.

Quantitative assessments of VEGF

ELISA and real-time qRT-PCR analyses were employed to assess the levels of VEGF proteins and mRNAs in the inner ears treated with 0.01, 0.1, or 1 mg/ml EP2 agonist, physiological saline, 0.01, 0.1, or 1 mg/ml EP4 agonist, or 0.01, 0.1, or 1% DMSO (n = 5 for each condition). ELISA analyses for VEGF proteins were performed using a mouse VEGF assay kit (Immuno-Biological Laboratories Co., Ltd., Takasaki, Japan) according to the manufacturer's protocol. All reactions were performed in triplicate.

For the real-time qRT-PCR analyses of *VEGF* mRNAs, the inner ear samples were homogenized with Trizol (Invitrogen), and total RNA was extracted using an RNeasy mini kit (Qiagen Ltd., Valencia, CA, USA). To eliminate genomic DNA contamination, the total RNA was treated with DNaseI (Ambion, Austin, TX, USA). The quantity and quality were evaluated using the A260/280 ratio and the appearance of the 18S and 28S ribosomal RNA bands upon electrophoresis. Complementary DNA (cDNA) was synthesized by reverse transcription

using TaqMan RT reagents (Applied Biosystems Inc., Foster City, CA, USA). The reactions were performed using a GeneAmp PCR system 9700 (Applied Biosystems Inc.) under the following conditions: 25°C for 10 min, 48°C for 30 min, 95°C for 5 min, and 4°C for 5 min. The primers used in the real-time qRT-PCR for *VEGF* and for the housekeeping gene glyceraldehydes 3-phosphate dehydrogenase (*GAPDH*) were as follows: 5'-ACTTGTGTTGGGAGGAGGA-3' (sense) and 5'-AAAGGACTTCGGCCTCTCT-3' (antisense) for *VEGF* (97 base pairs [bp]); and 5'-TGTGTCCGTCGTGGATCTGA-3' (sense) and 5'-CCTGCTTCACCACCTTCTTGAT-3' (antisense) for *GAPDH* (77 bp). The real-time qRT-PCR was performed at a final volume of 20 μl according to the manufacturer's protocols. The reaction mix comprised template cDNA, 10 μl POWER SYBR Green Master Mix (Applied Biosystems Inc.), a 0.5-μM final concentration of each primer, and ribonuclease-free water. The amplification conditions were as follows: 50°C for 2 min, 95°C for 10 min, 40 cycles of denaturation at 95°C for 15 s, and annealing at 60°C for 1 min. Fluorescence was detected with the ABI Prism 7000 sequence detection system (Applied Biosystems Inc.) and the associated software. Negative controls without template were included, and all reactions were performed in triplicate. The *VEGF* expression values were normalized to the housekeeping gene by dividing the mean of the *VEGF* triplicate value by the mean of the *GAPDH* triplicate value.

VEGF expression in cochleae

Immunohistochemistry was performed to examine the localization of VEGF in cochlear specimens treated with 0.1 mg/ml EP2 agonist, physiological saline, 0.1 mg/ml EP4 agonist, or 0.1% DMSO (n = 4 in each condition), and in non-treated cochleae (n = 3). Two mid modiolus sections from each cochlea were subjected to immunostaining for VEGF. Anti-mouse VEGF antibody (dilution, 5 μg/ml; R&D systems Inc., Minneapolis, MN, USA) was used as the primary antibody, and Alexa 488-conjugated donkey anti-goat IgG (dilution, 1:500; Invitrogen) was used as the secondary antibody. Kidney specimens obtained from the mice were used as positive controls. Nonspecific labeling was tested by omitting the primary antibody from the staining procedures.

VEGFR expression in cochleae

The expression of the VEGFRs Flt-1 and Flk-1 in normal cochleae (n = 4) was examined by immunohistochemistry. Anti-mouse Flt-1 antibody (dilution, 25 μg/ml; R&D Systems Inc.) and anti-mouse Flk-1 antibody (dilution, 15 μg/ml; R&D systems Inc.) were used as the primary antibodies, and Alexa 488-conjugated goat anti-rat IgG (dilution, 1:500; Invitrogen) and Alexa 488-conjugated donkey anti-goat IgG (dilution, 1:500; Invitrogen) were used as the secondary antibodies for Flt-1 and for Flk-1, respectively. The positive and negative controls were the same as those used in the VEGF immunostaining.

Statistical analysis

The differences in the levels of VEGF proteins among the samples treated with EP2 were examined using the one-factor analysis of variance with Scheffe's method. The differences in the levels of VEGF proteins between the samples treated with EP4 agonist and the control samples and those in the levels of and *VEGF* mRNAs between between the samples treated with EP2 or EP4 agonist and the control samples were examined using the unpaired *t*-test. A p value < 0.05 was considered statistically significant. All data are represented as the mean ± standard error.

Abbreviations

bp: base pairs; cAMP: cyclic adenosine monophosphate; cDNA: complementary DNA; DAPI: 4,6-diamidino, 2-phenylindole dihydrochloride; DMSO: dimethyl sulfoxide; EDTA: ethylenediamine tetra-acetic acid; ELISA: enzyme-linked immunosorbent assay; EP: prostaglandin E receptor subtype; Flk-1: fetal liver kinase-1; Flt-1: fms-related tyrosine kinase-1; *GAPDH*: glyceraldehyde 3-phosphate dehydrogenase; IgG: immunoglobulin G; mRNA: messenger RNA; PBS: phosphate-buffered saline; PFA: paraformaldehyde; PGE1: prostaglandin E1; PGE2: prostaglandin E2; PKA: protein kinase A; PSCC: posterior semicircular canal; qRT-PCR: quantitative reverse transcription-polymerase chain reaction; SNHL: sensorineural hearing loss; VEGF: vascular endothelial growth factor; VEGFR-1: vascular endothelial growth factor receptor-1; VEGFR-2: vascular endothelial growth factor receptor-2.

Authors' contributions

RH performed the experiments and data analyses, and contributed to manuscript preparation. TN coordinated and guided the experimental plans and contributed to manuscript writing. KH co-worked on the local application of EP agonists to the inner ear. NY and JI contributed to the conception of this study and participated in its design and execution. All authors contributed to and approved the final manuscript.

Acknowledgements

This work was supported by a Grant-in-Aid for Research on Sensory and Communicative Disorders from the Japanese Ministry of Health, Labor and Welfare. We thank Ono Pharmaceutical Co., Ltd. for providing ONO-AE1-259-01 and ONO-AE1-329.

Author Details

Department of Otolaryngology-Head and Neck Surgery, Graduate School of Medicine, Kyoto University, Kawaharacho 54, Shogoin, Sakyo-ku, 606-8507 Kyoto, Japan

Received: 2 October 2009 Accepted: 11 March 2010
Published: 11 March 2010

References

1. Wei BP, Mubiru S, O'Leary S: **Steroids for idiopathic sudden sensorineural hearing loss.** *Cochrane Database Syst Rev* 2006, **25**:CD003998.
2. Ogawa K, Takei S, Inoue Y, Kanzaki J: **Effect of prostaglandinE1 on idiopathic sudden sensorineural hearing loss: a doubleblinded clinical study.** *Otol Neurotol* 2002, **23**:665-668.
3. Ahn JH, Kim MR, Kim HC: **Therapeutic effect of lipoprostaglandin E1 on sudden hearing loss.** *Am J Otolaryngol* 2005, **26**:245-248.
4. Suzuki H, Fujimura T, Shiomori T, Ohbuchi T, Kitamura T, Hashida K, Udaka T: **Prostaglandin E1 versus steroid in combination with hyperbaric oxygen therapy for idiopathic sudden sensorineural hearing loss.** *Auris Nasus Larynx* 2008, **35**:192-197.

5. Zhuo XL, Wang Y, Zhuo WL, Zhang XY: **Is the application of prostaglandin E1 effective for the treatment of sudden hearing loss? An evidence-based meta-analysis.** *J Int Med Res* 2008, **36**:467-70.
6. Kiriyama M, Ushikubi F, Kobayashi T, Hirata M, Sugimoto Y, Narumiya S: **Ligand binding specificities of the eight types and subtypes of the mouse prostanoid receptors expressed in Chinese hamster ovary cells.** *Br J Pharmacol* 1997, **122**:217-224.
7. Narumiya S, Sugimoto Y, Ushikubi F: **Prostanoid receptors: structures, properties, and functions.** *Physiol Rev* 1999, **79**:1193-1226.
8. Coleman RA, Smith WL, Narumiya S: **International union of pharmacology classification of prostanoid receptors: properties, distribution and structure of the receptors and their subtypes.** *Pharmacol Rev* 1994, **46**:205-229.
9. Hori R, Nakagawa T, Sugimoto Y, Sakamoto T, Yamamoto N, Hamaguchi K, Ito J: **Prostaglandin E receptor subtype EP4 agonist protects auditory hair cells against noise-induced trauma.** *Neuroscience* 2009, **160**:813-819.
10. Inoue H, Takamori M, Shimoyama Y, Ishibashi H, Yamamoto S, Koshihara Y: **Regulation by PGE2 of the production of interleukin-6, macrophage colony stimulating factor, and vascular endothelial growth factor in human synovial fibroblasts.** *Br J Pharmacol* 2002, **136**:287-295.
11. Weiss TW, Mehrabi MR, Kaun C, Zorn G, Kastl SP, Speidl WS, Pfaffenberger S, Rega G, Glogar HD, Maurer G, Pacher R, Huber K, Wojta J: **Prostaglandin E1 induces vascular endothelial growth factor-1 in human adult cardiac myocytes but not in human adult cardiac fibroblasts via a cAMP-dependent mechanism.** *Mol Cell Cardiol* 2004, **36**:539-546.
12. Bradbury D, Clarke D, Seedhouse C, Corbett L, Stocks J, Knox A: **Vascular endothelial growth factor induction by prostaglandin E2 in human airway smooth muscle cells is mediated by E prostanoid EP2/EP4 receptors and SP-1 transcription factor binding sites.** *J Biol Chem* 2005, **28**:29993-30000.
13. Jain S, Chakraborty G, Raja R, Kale S, Kundu GC: **Prostaglandin E2 regulates tumor angiogenesis in prostate cancer.** *Cancer Res* 2008, **68**:7750-7759.
14. Gerber HP, Dixit V, Ferrara N: **Vascular endotheliul growth factor induces expression of the antiapoptotic proteins Bcl-2 and A 1 in vascular endothelial cells.** *J Biol Chem* 1998, **273**:13313-13316.
15. Cross MJ, Dixelius J, Matsumoto T, Claesson-Wslsh L: **VEGF-receptor signal transduction.** *Trends Biochem Sci* 2003, **28**:488-494.
16. Ferrara N, Gerber HP, LeCouter J: **he biology of VEGF and its receptors.** *Nat Med* 2003, **9**:669-676.
17. Ding XM, Mao BY, Jiang S, Li SF, Deng YL: **Neuroprotective effect of exogenous vascular endothelial growth factor on rat spinal cord neurons in vitro hypoxia.** *Chin Med J* 2005, **118**:1644-1650.
18. Góra-Kupilas K, Jośko J: **The neuroprotective function of vascular endothelial growth factor (VEGF).** *Folia Neuropathol* 2005, **43**:31-39.
19. Zachary I: **Neuroprotective role of vascular endothelial growth factor: signaling mechanisms, biological function, and therapeutic potential.** *Neurosignals* 2005, **14**:207-221. Review
20. Picciotti PM, Fetoni AR, Paludetti G, Wolf FI, Torsello A, Troiani D, Ferraresi A, Pola R, Sergi B: **Vascular endothelial growth factor (VEGF) expression in noise-induced hearing loss.** *Hear Res* 2006, **214**:76-83.
21. Selivanova O, Heinrich UR, Brieger J, Feltens R, Mann W: **Fast alterations of vascular endothelial growth factor (VEGF) expression and that of its receptors (Flt-1, Flk-1 and Neuropilin) in the cochlea of guinea pigs after moderate noise exposure.** *Eur Arch Otorhinolaryngol* 2007, **264**:121-128.
22. Quinn TP, Peters KG, De Vries C, Ferrara N, Williams LT: **Fetal liver kinase 1 is a receptor for vascular endothelial growth factor and is selectively expressed in vascular endothelium.** *Proc Natl Acad Sci USA* 2005, **90**:7533-7537.
23. Wen Y, Edelman JL, Kang T, Zeng N, Sachs G: **Two functional forms of vascular endothelial growth factor receptor-2/Flk-1 mRNA are expressed in normal rat retina.** *J Biol Chem* 1998, **273**:2090-2097.
24. Wang X, Klein RD: **Prostaglandin E2 induces vascular endothelial growth factor secretion in prostate cancer cells through EP2 receptor-mediated cAMP pathway.** *Mol Carcinog* 2007, **46**:912-923.
25. Sales KJ, Maudsley S, Jabbour HN: **Elevated prostaglandin EP2 receptor in endometrial adenocarcinoma cells promotes vascular endothelial growth factor expression via cyclic 3', 5'-adenosine monophosphate-mediated transactivation of the epidermal growth factor receptor and extracellular signal-regulated kinase 1/2 signaling pathway.** *Mol Endocrinol* 2005, **18**:1533-1545.
26. Rosenstein JM, Krum JM: **New roles for VEGF in nervous tissue--beyond blood vessels.** *Exp Neurol* 2004, **187**:246-253.
27. Michel O, Hess A, Bloch W, Schmidt A, Stennert E, Addicks K: **Immunohistochemical detection of vascular endothelial growth factor (VEGF) and VEGF receptors Flt-1 and KDR/Flk-1 in the cochlea of guinea pigs.** *Hear Res* 2001, **155**:175-180.
28. Picciotti P, Torsello A, Wolf FI, Paludetti G, Gaetani E, Pola R: **Age-dependent modifications of expression level of VEGF and its receptors in the inner ear.** *Exp Gerontol* 2004, **39**:1253-1258.
29. Picciotti PM, Torsello A, Cantore I, Stigliano E, Paludetti G, Wolf FI: **Expression of vascular endothelial growth factor and its receptors in the cochlea of various experimental animals.** *Acta Otolaryngol* 2005, **125**:1152-1157.
30. Shi X: **Cochlear pericyte responses to acoustic trauma and the involvement of hypoxia-inducible factor-1alpha and vascular endothelial growth factor.** *Am J Pathol* 2009, **174**:1692-1704.
31. Ogunshola OO, Antic A, Donoghue MJ, Fan SY, Kim H, Stewart WB, Madri JA, Ment LR: **Paracrine and autocrine functions of neuronal vascular endothelial growth factor (VEGF) in the central nervous system.** *J Biol Chem* 2002, **277**:11410-11415.
32. Holmes K, Roberts OL, Thomas AM, Cross MJ: **Vascular endothelial growth factor receptor-2: structure, function, intracellular signalling and therapeutic inhibition.** *Cell Signal* 2007, **19**:2003-2012.
33. Kitagawa K, Matsumoto M, Tagaya M, Hata R, Ueda H, Niinobe M, Handa N, Fukunaga R, Kimura K, Mikoshiba K, Kamada T: **"Ischemic tolerance" phenomenon found in the brain.** *Brain Res* 1990, **528**:21-24.
34. Miller BA, Perez RS, Shah AR, Gonzales ER, Park TS, Gidday JM: **Cerebral protection by hypoxic preconditioning in a murine model of focal ischemia-reperfusion.** *NeuroReport* 2001, **12**:1663-1669.
35. Lee HT, Chang YC, Tu YF, Huang CC: **VEGF-A/VEGFR-2 signaling leading to cAMP response element-binding protein phosphorylation is a shared pathway underlying the protective effect of preconditioning on neurons and endothelial cells.** *J Neurosci* 2009, **29**:4356-4368.
36. Canlon B, Fransson A: **Reducing noise damage by using a mid-frequency sound conditioning stimulus.** *Neuroreport* 1998, **9**:269-274.
37. Lee JE, Nakagawa T, Kim TS, Iguchi F, Endo T, Dong Y, Yuki K, Naito Y, Lee SH, Ito J: **A novel model for rapid induction of apoptosis in spiral ganglions of mice.** *Laryngoscope* 2003, **113**:994-999.
38. Nakagawa T, Kim TS, Murai N, Endo T, Iguchi F, Tateya I, Yamamoto N, Naito Y, Ito J: **A novel technique for inducing local inner ear damage.** *Hear Res* 2003, **176**:122-127.
39. Kada S, Nakagawa T, Ito J: **A mouse model for degeneration of the spiral ligament.** *J Assoc Res Otolaryngol* 2009, **10**:161-172.

doi: 10.1186/1471-2202-11-35
Cite this article as: Hori *et al.*, Role of prostaglandin E receptor subtypes EP2 and EP4 in autocrine and paracrine functions of vascular endothelial growth factor in the inner ear *BMC Neuroscience* 2010, **11**:35

The Laryngoscope

Sustained Delivery of Lidocaine Into the Cochlea Using Poly Lactic/Glycolic Acid Microparticles

Rie T. Horie, MD; Tatsunori Sakamoto, MD, PhD; Takayuki Nakagawa, MD, PhD; Yasuhiko Tabata, PhD, DMedSci, DPharm; Noboru Okamura, PhD; Naoki Tomiyama, PhD; Mitsuhiro Tachibana, MD; Juichi Ito, MD, PhD

Objectives/Hypothesis: Lidocaine is a local anesthetic that is known to suppress tinnitus via systemic or local application; however, this effect has only limited duration. The current study aimed to establish a method for the sustained delivery of lidocaine into the cochlea using poly lactic/glycolic acid (PLGA) microparticles.

Study Design: Experimental study.

Methods: Lidocaine-loaded PLGA microparticles were produced and their in vitro-release profiles were examined. The lidocaine concentrations in the perilymph were measured at different time points following the application of the lidocaine-loaded PLGA microparticles to the round-window membranes of guinea pigs. The possible adverse effects of the local application of lidocaine-loaded PLGA microparticles were also examined.

Results: The in vitro analyses revealed that the microparticles were capable of the sustained delivery of lidocaine. The in vivo experiments demonstrated the sustained delivery of lidocaine into the cochlear fluid, and the maintenance of high lidocaine concentrations in the perilymph for up to 3 days after application. Nystagmus and inflammation in the middle ear mucosa were not detected after the local application of lidocaine-loaded PLGA microparticles, although temporary hearing loss was observed.

Conclusions: Lidocaine-loaded PLGA microparticles were shown to be capable of the sustained delivery of lidocaine into the cochlea, suggesting that they could be used for the attenuation of peripheral tinnitus.

Key Words: Biomaterial, drug-delivery system, inner ear, poly lactic/glycolic acid, tinnitus.

***Laryngoscope*, 000:000–000, 2010**

INTRODUCTION

Tinnitus is the perception of sound within the human ear in the absence of corresponding external stimuli. Tinnitus is not a disease, but rather a symptom resulting from a range of underlying causes. It can be a serious problem for patients, because it can lead to severe depression with negative effects on the activities of daily life. Tinnitus is encountered by otolaryngologists worldwide; however, at present, only limited treatment options are available. Many different drugs have been used for the treatment of tinnitus, but with little success. One of the major obstacles to developing efficient treatments for tinnitus is the fact that tinnitus has various forms and underlying mechanisms. Theories about tinnitus pathophysiology emphasize abnormal peripheral or central neural activity in the auditory system.[1]

Several studies have reported on the efficacy of the local or systemic administration of lidocaine,[2–4] which is the most commonly used local anesthetic and is also employed as an antiarrhythmic agent. Various reports have suggested the cochlea, auditory nerve, and central auditory pathway as sites of lidocaine action on tinnitus.[5] Several studies have shown that the systemic application of lidocaine can alleviate tinnitus; however, this effect has only limited duration, and the treatment carries a risk of serious side effects, including cardiac

From the Department of Otolaryngology, Head and Neck Surgery, Graduate School of Medicine (R.T.H., T.S., T.N., J.I.), the Department of Pathology and Biology of Diseases (M.T.), the Department of Diagnostic Pathology, Graduate School of Medicine (M.T.), the Department of Biomaterials, Institute for Frontier Medical Sciences (Y.T.), Kyoto University, Kyoto; and the Department of Pharmaceutical Sciences, Mukogawa Woman's University, Nishinomiya (N.O., N.T.), Japan.

Editor's Note: This Manuscript was accepted for publication May 12, 2009.

Presented at the 31st Midwinter Research Meeting of Association for Research in Otolaryngology, Phoenix, Arizona, U.S.A., February 16–21, 2008; the 32nd Midwinter Research Meeting of Association for Research in Otolaryngology, Baltimore, Maryland, U.S.A., February 14–19, 2009; and the 45th Workshop on Inner Ear Biology, Ferrara, Italy, September 21–24, 2008.

This study was supported by a Grant-in-Aid for Research on Sensory and Communicative Disorders, a Grant-in-Aid for Research on Nanotechnological Medical from the Ministry of Health, Labour and Welfare of Japan, and by a grant from the Tinnitus Research Initiative.

Send correspondence to Takayuki Nakagawa, MD, PhD, Department of Otolaryngology, Head and Neck Surgery, Graduate School of Medicine, Kyoto University, Kawaharacho 54, Shogoin, Sakyo-ku, Kyoto 606-8507, Kyoto, Japan. E-mail: tnakagawa@ent.kuhp.kyoto-u.ac.jp

DOI: 10.1002/lary.20713

arrhythmia and central nervous system excitation or depression.[2] The local application of lidocaine into the intratympanic space can avoid such systemic toxicity, but causes vertigo or dizziness.[4] Tinnitus suppression by local lidocaine application also has limited duration.[3]

Rapid recent technological progression has made possible the sustained and/or targeted delivery of drugs. We have developed a local system for the sustained delivery of growth factors for the treatment of inner ear disorders.[6] Local application can eliminate systemic side effects and deliver drugs to targeted organs at high concentrations. The use of drug-delivery systems in local treatment prolongs the therapeutic effects, and is sometimes necessary to achieve biological effects. We proposed that the use of drug-delivery systems for local lidocaine application could help to prolong the suppression of tinnitus caused by cochlear dysfunction. The current study thus aimed to develop a system for the sustained delivery of lidocaine to the cochlea, and to examine the possible adverse effects. Poly lactic/glycolic acid (PLGA), which is a material used for absorbable sutures, was investigated as a biomaterial for the sustained delivery of lidocaine. PLGA microparticles encapsulating lidocaine were produced, and their release profiles were examined both in vitro and in vivo. The effects on hearing, vestibular function, and histology of the middle ear mucosa were determined to evaluate the risk of adverse effects.

MATERIALS AND METHODS

Animals

Hartley guinea pigs (female; weight, 300–500 g; N = 74) were purchased from Japan SLC Inc. (Shizuoka, Japan). The Animal Research Committee of the Graduate School of Medicine, Kyoto University, Kyoto, Japan, approved all experimental protocols. Animal care was supervised by the Institute of Laboratory Animals of the Graduate School of Medicine, Kyoto University. All experimental procedures were performed in accordance with the National Institutes of Health, Guidelines for the Care and Use of Laboratory Animals.

Preparation of Lidocaine-Loaded PLGA Microparticles

PLGA with a lactic/glycolic acid ratio of 70:30 (molecular weight, 10,000 Daltons) was obtained from Polysciences Inc. (Warrington, PA). Polyvinyl alcohol (PVA), UP180 (degree of polymerization, 1,800), and UMR10H (degree of polymerization, 250) were purchased from Japan Vam & Plval Co., Ltd. (Osaka, Japan). Lidocaine powder and phosphate buffered saline (PBS) were purchased from Nacalai Tesque (Kyoto, Japan). Acetonitrile and Tween-80 were purchased from Tokyo Chemical Industry Co., Ltd. (Tokyo, Japan). Dichloromethane (DCM) was purchased from Fisher Scientific (Tokyo, Japan). All solvents were high-performance liquid chromatography (HPLC) grade.

Microparticles were prepared using emulsification by the homogenization-solvent evaporation method. Briefly, an organic phase was prepared consisting of the polymer (PLGA) and the drug (lidocaine), dissolved in an organic solvent (DCM). The organic phase was added to an aqueous phase containing a surfactant (PVA) to form an emulsion. This was broken down into microdroplets by applying external energy, and the droplets formed microparticles on solvent evaporation.

The effect of lidocaine loading on the release profile was examined in two kinds of PLGA microparticles. The microparticles were produced using 2 g PLGA or 2 g lidocaine dissolved in 5.5 mL DCM, or 500 mg PLGA or 500 mg lidocaine dissolved in 5 mL DCM, respectively. The organic phase was then mixed with 50 mL of 1% (wt/wt) PVA solution, and 50 mL of 1% (wt/wt) PVA solution was added as the aqueous phase. This was followed by stirring at 5,000 rpm for 5 minutes, and evaporation of the solvent for 3 days. The microparticles were collected by centrifugation at 5,000 rpm and 4°C, and then freeze dried. The lidocaine-free microparticles were prepared using a similar method, but in the absence of lidocaine. The surface morphology and average particle diameters of the microparticles were examined by scanning electron microscopy (SEM). The average size was estimated from the diameter of 100 randomly selected microparticles. Finally, lidocaine-loaded large (Lido-L) microparticles and lidocaine-loaded small (Lido-S) microparticles were prepared.

The lidocaine loading contents of the Lido-L and Lido-S microparticles were analyzed by the method reported previously.[7] The concentration of lidocaine in the supernatant was measured by an ultraviolet (UV) detector (wavelength, 263 nm), and the total amount of lidocaine in the particles was determined. The lidocaine contents (%) were calculated as follows: (weight of lidocaine in microparticles)/(total weight of microparticles)×100. Three independent measurements were performed for each condition.

In Vitro-Release Profile

The lidocaine-release profiles of the Lido-L and Lido-S microparticles were determined in vitro. A 2.5-mg sample of the microparticles was incubated in a tube containing 1.5 mL PBS (pH 7.4) with 0.2% (wt/wt) Tween-80 buffer. The samples were then placed in a shaken water bath regulated at 30 rpm and 37°C. Sampling of 1 mL of the buffer was performed at 1, 2, 4, 6, and 12 hours, and 4, 7, 14, 21, 28, and 32 days after incubation, followed by replacement with 1 mL of fresh buffer. The concentration of lidocaine in the samples was determined using a UV detector (wavelength, 263 nm). The cumulative amount of lidocaine released was calculated for each time point. The lidocaine-release profile of each particle (%) was calculated as follows: (cumulative amount of lidocaine released)/(total lidocaine content)×100. The amounts of released lidocaine per hour were also calculated for the following time points: 0 to 1 hour, 1 to 2 hours, 2 to 4 hours, 4 to 6 hours, 6 to 12 hours, 12 hours to 4 days, 4 to 7 days, 7 to 14 days, and 14 to 21 days. Three independent measurements were performed for each condition.

In Vivo-Release Profile

The lidocaine concentration in the perilymph was measured on days 1, 3, 7, and 14 after the application of 2.5 mg Lido-L microparticles to the round-window membrane (RWM) of the guinea pigs (n = 16). The animals were anesthetized with an intramuscular injection of midazolam (5 mg/kg; Astellas Co., Tokyo, Japan), medetomidine (18.5 μg/kg; Zenoac, Fukushima, Japan), and butorphanol tartrate (0.25 mg/kg; Bristol-Myers, K.K., Tokyo, Japan). A small hole was made in the bulla to expose the cochlea, and Lido-L microparticles were placed on the RWM. To measure the lidocaine concentrations in the perilymph, the cochleae were excised from the temporal bones under general anesthesia on day 1 (n = 7), day 3 (n = 4), day 7 (n = 6), and day 14 (n = 4). Each cochlea was punctured at the apical portion, and 3 μL perilymph was aspirated using a 30-gauge needle (BD and Company, Fukuoka, Japan). The perilymph samples collected from the animals on day 1 after the sham-operation (n = 4) were used as a negative control.

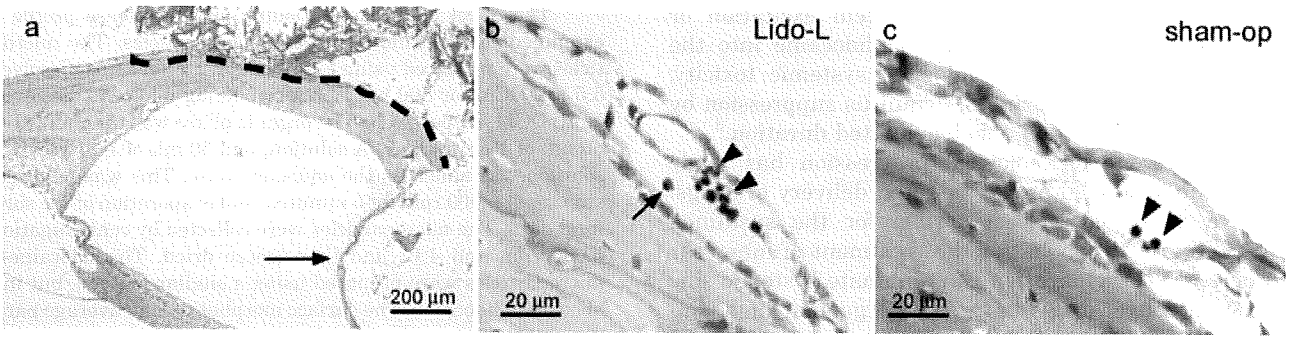

Fig. 1. Histopathology of the middle ear mucosa 7 days after local application of Lido-L microparticles (Lido-L) or sham-operation (sham-op). (a) The dotted line indicates the evaluated area of the middle ear mucosa. The arrow shows the RWM. (b) The middle ear mucosa treated with Lido-L microparticles showed a few lymphocytes (arrowheads) and a neutrophil (an arrow). (c) A few lymphocytes (arrowheads) were found in a sham-operated specimen.

The concentration of lidocaine in the perilymph was measured by reverse-phase (RP)-HPLC using the Shiseido Nanospace SI-2 system (Shiseido, Tokyo, Japan). The lidocaine was separated on a Cosmosil C_{18}-AR-II reverse-phase column (5 μm, 4.6 mm I.D. $\times$ 150 mm; Nacalai Tesque, Kyoto, Japan) at 35°C. The mobile phase consisted of water (0.1 M NaH_2PO_4/Na_2HPO_4, pH adjusted to 4.5) and methanol at a volume ratio of 40:60. The flow rate was 0.3 mL/minute. The detector potential was maintained at +1.0 V.

Effects on Auditory Function

To assess the effects of the local application of Lido-L microparticles on the auditory function, the auditory brainstem response (ABR) was recorded. Lido-L microparticles (2.5 mg) were placed on the left RWM of guinea pigs (n = 4) under general anesthesia. Lidocaine-free PLGA particles were applied to the controls (n = 4). ABR measurements were performed preoperatively (day 0), and on days 1, 3, 7, and 14 after application, according to previous studies.[6]

Effects on Vestibular Function

Vestibular dysfunction was assessed by the occurrence of nystagmus after the local application of either Lido-L microparticles (n = 16) or a piece of gelatin sponge immersed with 20 μL of 0.5%, 1%, 2%, or 4% lidocaine hydrochloride (Astra Zeneca K.K., Osaka, Japan; n = 2 for each concentration of lidocaine). The Lido-L microparticles (2.5 mg) or pieces of gelatin sponge immersed with lidocaine hydrochloride were placed on the RWM of the right ear under general anesthesia with sevoflurane (Abbott Japan Co., Ltd., Tokyo, Japan). The direction and the duration of nystagmus were recorded using an infrared video system in a dark room for 2 hours. In addition, for the Lido-L microparticle-treated animals, the occurrence of nystagmus was evaluated on days 1, 3, and 7 after application. The concentrations of lidocaine in the perilymph were also measured 5 minutes after the local application of 1% or 2% lidocaine hydrochloride (n = 4 for each concentration of lidocaine). The concentration of lidocaine was analyzed using the method described for the in vivo-release profile.

Inflammatory Responses

The inflammatory responses in the middle ear following the local application of Lido-L microparticles were estimated histologically. On day 7 after the local application of Lido-L microparticles (2.5 mg) to the RWM of guinea pigs, the temporal bones were collected and fixed with 4% paraformaldehyde in PBS at pH 7.4 for 3 hours at room temperature (n = 4). Specimens obtained from sham-operated animals (n = 4), which underwent surgical procedures without substances being applied to the RWM, served as controls. The paraffin-embedded tissues were processed into 3 μm sections, and stained with hematoxylin and eosin. Two midmodiolar sections from each cochlea were subjected to quantitative analyses. The numbers of lymphocytes, neutrophils, and plasmacytes in the middle ear mucosa were counted in five randomly selected fields located within 1 mm of the edge of the RWM under a $\times$40 objective lens for each section (Fig. 1a). The distance from the edge of the RWM was measured using Image J software (http://www.nist.gov/lispix/imlab/prelim/dnld.html). Cell counting was performed in a blind manner. The average cell number in five fields was used for each animal in the analysis.

Statistical Analyses

The differences in lidocaine concentrations among time points after Lido-L microparticle application were examined by analysis of variance (ANOVA) with the Tukey-Kramer test. The overall effect of the local application of Lido-L or lidocaine-free PLGA microparticles on the ABR thresholds was examined by 2-way factorial ANOVA. When the interactions were significant, multiple comparisons using the Tukey-Kramer test were performed for pair-wise comparisons. The numbers of infiltrated cells in the middle ear mucosa of the Lido-L microparticle-treated animals were compared with those in the sham-operated animals using the unpaired t test. A P value <0.05 was considered statistically significant. All data are represented as the mean $\pm$ standard error.

RESULTS

In Vitro-Release Profile

SEM demonstrated that the Lido-L and Lido-S microparticles had a smooth and round surface morphology (Fig. 2). The average outer diameter of the Lido-L microparticles was 100.0 $\pm$ 3.0 μm, and that of the Lido-S microparticles was 5.0 $\pm$ 0.5 μm, indicating their stable production. The loading contents of lidocaine were 41.8% $\pm$ 1.1% for the Lido-L microparticles and 5.0% $\pm$ 0.1% for the Lido-S microparticles. In general, the drug-release profiles of PLGA particles are partitioned into four phases: an initial burst period (phase 1), an induction period (phase 2), a slow-release period (phase 3), and a final release period (phase 4). The cumulative release

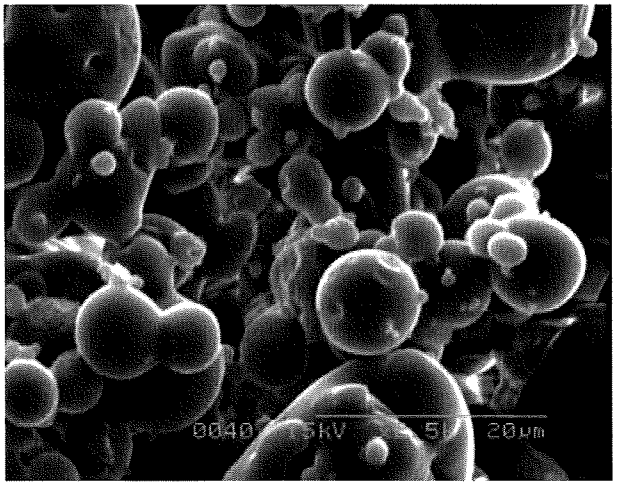

Fig. 2. Surface morphology of lidocaine-loaded microparticles. The scale bar represents 20 μm.

profiles of lidocaine from the Lido-L and Lido-S microparticles are shown in Figure 3a. A burst period (phase 1) was observed for both types of microparticle at 24 hours, which was followed by phase 2. The Lido-L microparticles released 77.3% ± 2.3% of the lidocaine contents during phases 1 and 2 (days 0–7). By the end of phase 3 (days 7–56), 82.7% ± 3.3% of the lidocaine had been released. A final release period was not observed during the experimental period. The Lido-S microparticles released 76.6% ± 1.0% of the lidocaine during phases 1 and 2 (days 0–7). By the end of phase 3 (days 7–21), 94.7% ± 0.9% of the lidocaine had been released, and by the end of phase 4 (days 21–56) the amounts reached up to 98.9% ± 0.9%. The amounts of lidocaine released per hour from the Lido-L and Lido-S microparticles are shown in Figure 3b. The Lido-L microparticles exhibited the stable release of lidocaine during the initial 12 hours. In the first hour, lidocaine was released from these microparticles at a rate of 669.8 μg/hour. Between 1 and 6 hours, over 200 μg/hour lidocaine was released, whereas the rate fell to 79.7 μg/hour between 6 and 12 hours. Lidocaine was released at a rate of 10.5 μg/hour between 12 hours and 4 days, and this decreased to 2.4 μg/hour between 4 and 7 days. By contrast, the Lido-S microparticles released lidocaine at a rate below 30 μg/hour, even between 1 and 2 hours. These findings indicated that the Lido-S microparticles released the majority of the loaded lidocaine in an initial burst, which was not advantageous for sustained release. By contrast, the Lido-L microparticles showed the continuous release of comparatively large amounts of lidocaine during the initial 12 hours, indicating that local application might maintain high concentrations of lidocaine in the cochlear fluid for a few days. We therefore used Lido-L microparticles in the subsequent experiments.

In Vivo-Release Profile

RP-HPLC analyses demonstrated measurable concentrations of lidocaine in the perilymph samples collected from the cochleae 1 to 14 days after Lido-L microparticle application to the RWM (Fig. 4). The lidocaine concentrations were 744.0 ± 176.9 ng/mL on day 1, and 863.3 ± 366.3 ng/mL on day 3. The values decreased to 87.2 ± 27.2 ng/mL on day 7, and were maintained at 30.3 ± 13.6 ng/mL on day 14. The difference in lidocaine concentrations between days 3 and 7 was statistically significant (Tukey-Kramer test). These findings demonstrated that the lidocaine released from Lido-L microparticles was transferred into the perilymph through the RWM, and that high concentrations of lidocaine in the perilymph were maintained for at least 3 days, which was consistent with the in vitro-release profiles of the Lido-L microparticles.

Effects on Auditory Function

The ABR thresholds after the application of Lido-L or lidocaine-free microparticles are shown in Figure 5.

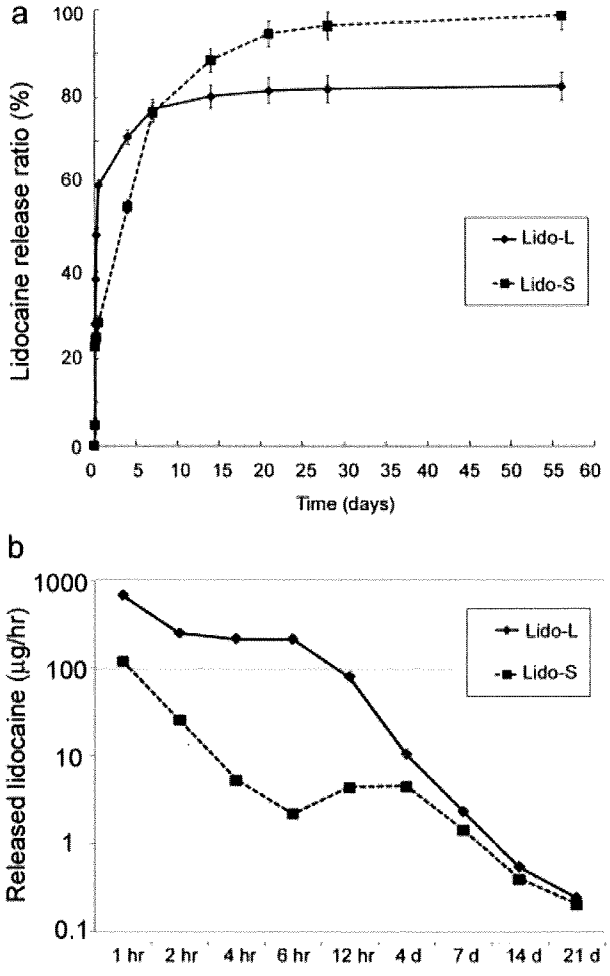

Fig. 3. In vitro-release profiles of lidocaine from Lido-L and Lido-S microparticles. The closed squares show the data for Lido-S microparticles, and the closed diamonds show the data for Lido-L microparticles. (a) Cumulative amounts of lidocaine released from Lido-L or Lido-S microparticles at each time point. The value (%) was calculated as follows: (cumulative amount of lidocaine released)/(total lidocaine content)×100. (b) The amount of lidocaine released per hour at the following time points: 0 to 1 hour, 1 to 2 hours, 2 to 4 hours, 4 to 6 hours, 6 to 12 hours, 12 hours to 4 days, 4 to 7 days, 7 to 14 days, and 14 to 21 days.

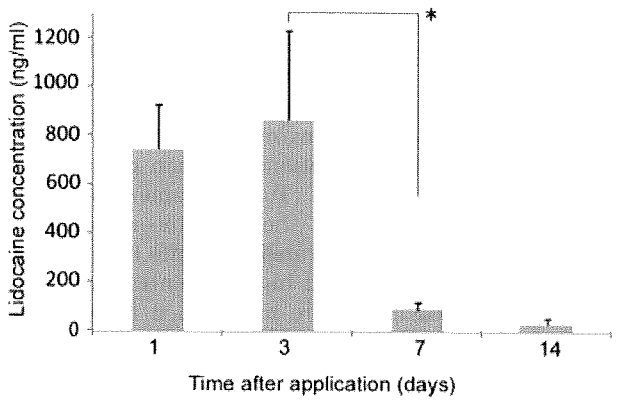

Fig. 4. Lidocaine concentrations in the perilymph following local application of Lido-L microparticles. The bars represent the standard errors. *Significant difference by analysis of variance with the Tukey-Kramer test.

Interestingly, the animals treated with Lido-L microparticles showed a temporal elevation of the ABR thresholds on day 7 at each frequency, although the lidocaine concentration in the perilymph decreased significantly at this time point. The overall effects of Lido-L microparticle application on the ABR thresholds were statistically significant in comparison with those in animals treated with lidocaine-free particles (4 kHz, $P = .0295$; 8 kHz, $P = .0016$; and 16 kHz, $P = .001$). In the Lido-L microparticle-treated animals, pair-wise comparisons demonstrated significant differences in the ABR thresholds between day 7 and before or day 1 or 14 at 4 and 8 kHz, and between day 7 and before or day 1 at 16 kHz (Fig. 5). By contrast, the animals administered lidocaine-free particles showed no significant differences among the time points. The differences in the ABR thresholds between the Lido-L microparticle-treated and lidocaine-free particle-treated animals were significant on day 7 at all tested frequencies (Fig. 5).

Effects on Vestibular Function

Before testing the Lido-L microparticles, we measured the duration of nystagmus following the local application of lidocaine hydrochloride at various concentrations, and the lidocaine concentration in the perilymph 15 minutes after the local application of 1% or 2% lidocaine hydrochloride, to examine the efficacy of our system for the estimation of nystagmus. The local application of 0.5% lidocaine hydrochloride did not cause nystagmus. However, nystagmus was induced in the animals treated with 1%, 2%, or 4% lidocaine hydrochloride. The latency time was 2 minutes with 1%, 2%, or 4% lidocaine hydrochloride treatment, and nystagmus with horizontal components developed toward the treated side for approximately 10 minutes. The nystagmus then gradually disappeared in the animals treated with 1% lidocaine hydrochloride. In those treated with 2% or 4% lidocaine hydrochloride, paralytic nystagmus with horizontal components developed toward the opposite side and persisted for over 2 hours. RT-HPLC analyses showed that the lidocaine concentrations in the perilymph were 10,708 ± 4,606 ng/mL after the application of 1% lidocaine hydrochloride and 17,384 ± 4,027 ng/mL after the application of 2% lidocaine hydrochloride. These findings confirmed that our system detected the nystagmus induced by lidocaine delivered into the cochlear fluid. We then examined the occurrence of nystagmus following local Lido-L microparticle application in 16 animals. Nystagmus and abnormal behaviors indicating vestibular dysfunction were not observed in any of these guinea pigs.

Inflammatory Responses

No severe inflammatory responses, including effusion or swelling of the mucosa, were identified in either Lido-L microparticle-treated or sham-operated ears. However, inflammatory cells were present in the middle

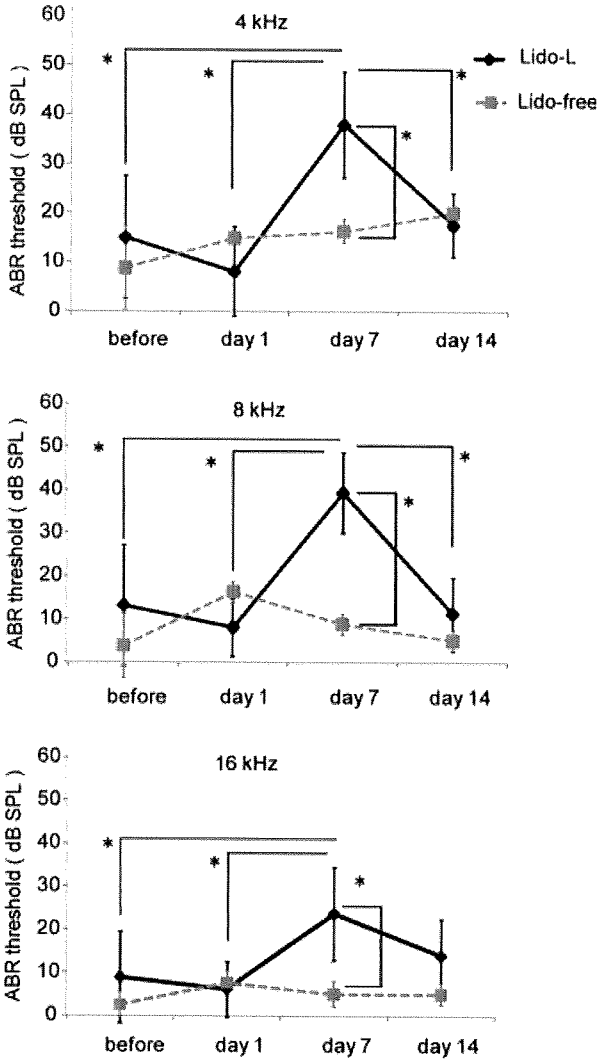

Fig. 5. Auditory brainstem response (ABR) thresholds 4, 8, and 16 kHz before and after local application of Lido-L microparticles or lidocaine-free poly lactic/glycolic acid microparticles. The closed diamonds show the data for Lido-L microparticles (Lido-L), and the closed squares show the data for lidocaine-free particles (Lido-free). *Significant differences according to the Tukey-Kramer test.

ear mucosa of both groups (Fig. 1b, 1c). The numbers of lymphocytes, neutrophils, and plasmacytes in the Lido-L microparticle-treated specimens were 15.3 ± 3.6, 2.8 ± 1.2, and 6.8 ± 1.3, and those in the sham-operated specimens were 16.0 ± 2.8, 4.8 ± 1.1, and 7.3 ± 2.5, respectively. There were no significant differences in the numbers of lymphocytes, neutrophils, or plasmacytes between the Lido-L microparticle-treated and sham-operated specimens.

DISCUSSION

The analyses of the in vitro-release profiles demonstrated that the Lido-L microparticles released lidocaine in a typical sustained-release fashion, whereas the Lido-S microparticles released the majority of the loaded lidocaine during an initial burst. The lidocaine concentrations in the perilymph after the local application of Lido-L microparticles to the guinea pig cochleae demonstrated sustained delivery into the cochlear fluid. High amounts of lidocaine in the perilymph were found a couple of days after the local application, and measurable concentrations were still present after 14 days. These findings demonstrated that Lido-L microparticles were capable of sustained lidocaine delivery into the perilymph after application to the guinea pig RWM.

Local lidocaine application has the advantage of the elimination of systemic side effects compared with systemic lidocaine application. However, local application has side effects including vestibular dysfunction. We examined the occurrence of nystagmus to evaluate the risk of vestibular dysfunction following the local application of Lido-L microparticles. Nystagmus was not observed after the local application of Lido-L microparticles to guinea pigs, although the local application of 2% or 4% lidocaine hydrochloride caused severe nystagmus, as previously reported in rats.[8] The deficit of nystagmus after local application of Lido-L microparticles may be due to a lower concentration of lidocaine in the perilymph than that necessary for anesthetic actions on vestibular peripheral systems. We also examined the inflammatory responses in the middle ear mucosa of guinea pigs following the local application of Lido-L microparticles. No significant infiltration of inflammatory cells was observed in the Lido-L microparticle-treated specimens compared with the sham-operated specimens. Local application using lidocaine-loaded PLGA microparticles, therefore, appeared to be a safe strategy for the sustained delivery of lidocaine into the cochlear fluid.

The present study demonstrated interesting effects of the local application of Lido-L microparticles on hearing. ABR recordings showed a temporal elevation of thresholds on day 7 after application, but no permanent threshold shifts. Histological analyses revealed no significant damage to the middle ear mucosa on day 7 after the local application of Lido-L microparticles, indicating that the observed ABR threshold shifts were not conductive hearing loss. In the ABR recording experiments, lidocaine-free PLGA particles were applied locally to control animals, which showed no significant alterations in the ABR thresholds. The temporal elevation of ABR thresholds observed on day 7 might have been caused by the effects of sustained lidocaine delivery into the cochlear fluid on the auditory pathway. These findings demonstrate that the local application of Lido-L microparticles have certain effects on the auditory system, which can be associated with a beneficial (silencing tinnitus), or an adverse effect (progression of hearing impairment). We should precisely examine the risk for progression of hearing impairment by local application of Lido-L microparticles before clinical application.

The therapeutic effects of lidocaine on the Purkinje fibers in the heart are generally associated with plasma levels of 6 to 25 μM (1.5–6 μg freebase per mL).[9] In general, the suppression of tinnitus by systemic lidocaine application has occurred at equal or lower plasma levels of lidocaine. The present findings demonstrated that the lidocaine concentrations in the perilymph during the initial 3 days after application were maintained at approximately 0.8 μg freebase per mL. We therefore propose that the concentrations of lidocaine in the perilymph after the local application of Lido-L microparticles might be sufficient for tinnitus suppression if the targets are located in the cochlea. Experimental studies have indicated that the spiral ganglion neurons might be one origin of tinnitus in the cochlea.[10] Lidocaine is known to cause the failure of depolarization in neurons by blocking sodium channels, resulting in anesthetic effects. The anesthetic effects of lidocaine on the spiral ganglion neurons require local lidocaine application at a concentration of over 40 mM (1% lidocaine hydrochloride).[11] In the present study, 15 minutes after the local application of 1% lidocaine hydrochloride, the concentration of lidocaine in the perilymph reached 10 μg/mL, which was higher than the maximum concentration of lidocaine following local Lido-L microparticle application. However, a study using ^{14}C-lidocaine demonstrated the accumulation of lidocaine in the cochlear modiolus, where the spiral ganglion neurons are located, after the systemic application of lidocaine.[12] It is therefore possible that locally applied lidocaine accumulates in the spiral ganglion neurons, which could explain the temporal threshold shifts observed on day 7 in the present study. However, lidocaine also affects various types of channel and receptor, including potassium channels and N-methyl-D-aspartic acid (NMDA) receptors.[5] The blocking of potassium currents by lidocaine occurs in the outer hair cells, leading to the reduction of cochlear microphonics.[13] The involvement of NMDA receptors in the generation of peripheral tinnitus has also been indicated in an animal model.[14] Hence, further studies are needed to elucidate the mechanisms of lidocaine action in the cochlea.

CONCLUSION

We produced lidocaine-loaded PLGA microparticles that were capable of the sustained delivery of lidocaine into the cochlea after local application to the RWM. The local application of lidocaine-loaded PLGA microparticles had no significant adverse effects, including vertigo and

otitis media, although the ABR thresholds were temporally elevated. These findings suggest a potential use of lidocaine-loaded PLGA microparticles for the attenuation of peripheral tinnitus. The established animal models of tinnitus[15] could be used to test the efficacy of lidocaine-loaded PLGA microparticles for the attenuation of peripheral tinnitus. In addition, it is also crucial to develop methods for diagnosis of peripheral tinnitus before clinical application.

Acknowledgment

We would like to thank Toshihiro Ogawa, Naoki Hayashi, and Masataka Yoshida for their technical contributions.

BIBLIOGRAPHY

1. Bauer CA. Mechanisms of tinnitus generation. *Curr Opin Otolaryngol Head Neck Surg* 2004;12:413–417.
2. Murai K, Tyler RS, Harker LA, Stouffer JL. Review of pharmacologic treatment of tinnitus. *Am J Otol* 1992;13: 454–464.
3. Delucchi E. Transtympanic pilocaine in tinnitus. *Int J Tinnitus* 2000;6:37–40.
4. Sakata H, Kojima Y, Koyama S, Furuya N, Sakata E. Treatment of cochlear tinnitus with transtympanic infusion of 4% lidocaine into the tympanic cavity. *Int J Tinnitus* 2001;7:46–50.
5. Trellakis S, Lautermann J, Lehnerdt G. Lidocaine: neurobiological targets and effects on the auditory system. *Prog Brain Res* 2007;166:303–322.
6. Lee KY, Nakagawa T, Okano T, et al. Novel therapy for hearing loss: delivery of insulin-like growth factor 1 to the cochlea using gelatin hydrogel. *Otol Neurotol* 2007; 28:976–981.
7. Chen PC, Park YJ, Chang LC, et al. Injectable microparticle-gel system for prolonged and localized lidocaine release. I. In vitro characterization. *J Biomed Mater Res A* 2004;70:412–419.
8. Magnusson AK, Tham R. Vestibulo-oculomotor behaviour in rats following a transient unilateral vestibular loss induced by lidocaine. *Neuroscience* 2003;120:1105–1114.
9. Thomson PD, Melmon KL, Richardson JA, et al. Lidocaine pharmacokinetics in advanced heart failure, liver disease, and renal failure in humans. *Ann Intern Med* 1973;78: 499–508.
10. Tan J, Ruttiger L, Panford-Walsh R, et al. Tinnitus behavior and hearing function correlate with the reciprocal expression patterns of BDNF and Arg3.1/arc in auditory neurons following acoustic trauma. *Neuroscience* 2007; 145:715–726.
11. Laurikainen E, Nuttall AL, Miller JM, Quirk WS, Virolainen E. Experimental basis for lidocaine therapy in cochlear disorders. *Acta Otolaryngol* 1992;112:800–809.
12. Englesson S, Larsson B, Lindquist NG, Lyttkens L, Stahle J. Accumulation of 14C-lidocaine in the inner ear. Preliminary clinical experience utilizing intravenous lidocaine in the treatment of severe tinnitus. *Acta Otolaryngol* 1976;82:297–300.
13. Laurikainen E, Lin X, Nuttall AL, Dolan DF. The mechanism and site of action of lidocaine hydrochloride in guinea pig inner ear. *Acta Otolaryngol* 1997;117:523–528.
14. Ruel J, Chabbert C, Nouvian R, et al. Salicylate enables cochlear arachidonic-acid-sensitive NMDA receptor responses. *J Neurosci* 2008;28:7313–7323.
15. Turner JG. Behavioral measures of tinnitus in laboratory animals. *Prog Brain Res* 2007;166:147–156.

Molecular and Cellular Neuroscience 42 (2009) 391–398

Contents lists available at ScienceDirect

Molecular and Cellular Neuroscience

journal homepage: www.elsevier.com/locate/ymcne

Silencing p27 reverses post-mitotic state of supporting cells in neonatal mouse cochleae

Kazuya Ono [a], Takayuki Nakagawa [a,*], Ken Kojima [a], Masahiro Matsumoto [a], Takeshi Kawauchi [b], Mikio Hoshino [c], Juichi Ito [a]

[a] Department of Otolaryngology, Head and Neck Surgery, Graduate School of Medicine, Kyoto University, Kawaharacho 54, Shogoin, Sakyo-ku, 606-8507 Kyoto, Japan
[b] Department of Anatomy, Keio University School of Medicine, 160-8582 Tokyo, Japan
[c] Department of Biochemistry and Cellular Biology, National Institute of Neuroscience, National Center of Neurology and Psychiatry, 187-8502 Tokyo, Japan

ARTICLE INFO

Article history:
Received 8 May 2009
Revised 30 July 2009
Accepted 30 August 2009
Available online 4 September 2009

Keywords:
RNA interference
Cyclin-dependent kinase inhibitor
Cochlea
Mitosis
Apoptosis
Regeneration

ABSTRACT

The post-natal cochlear mammalian epithelium have no capacity to proliferate in tissue, however, dissociated supporting cells exhibit the ability to divide and trans-differentiate into new hair cells *in vitro*, with this process found to be correlated with the downregulation of the cyclin-dependent kinase inhibitor $p27^{kip1}$. Here we show that knockdown of $p27^{kip1}$ with short hairpin RNA-expressing vectors results in the cell-cycle reentry of post-mitotic supporting cells in the post-natal mouse cochleae *ex vivo*. The $p27^{kip1}$-knockdown cells incorporated BrdU, and then divided into two daughter cells. However, there was also activation of the apoptotic pathway in some supporting cells. These results indicate that the use of RNA interference to target $p27^{kip1}$ is an effective strategy for inducing cell-cycle reentry in post-mitotic supporting cells in the post-natal mammalian cochleae, although additional manipulations of the supporting cells are required to achieve hair cell regeneration.

Introduction

Sensorineural hearing loss (SNHL) is one of the most common disabilities. Auditory hair cells in the cochlea are mechanoreceptors that play a crucial role in hearing. In mammals, if the hair cells are damaged or lost, the resulting SNHL is permanent. Therefore, one of the best approaches for improving hearing in mammals would be to find a way to induce hair cell regeneration.

The cochlear epithelium is composed of hair cells and supporting cells (SCs). In the avian auditory epithelium, SCs are able to reenter the cell cycle and proliferate in response to hair cell loss, which gives rise to both new hair cells and SCs (Corwin and Cotanche, 1988; Ryals and Rubel, 1988). In mice, progenitors of the cochlear epithelium stop dividing by embryonic day 14.5 (Ruben, 1967), with differentiation of the hair cells and SCs occurring after this terminal mitosis. Both hair cells and SCs maintain a post-mitotic state throughout life in adult mammals, and do not exhibit any spontaneous capacity to divide under normal conditions or in response to damage *in vivo* (Roberson and Rubel, 1994).

It has been determined that the cyclin-dependent kinase inhibitor (CKI), $p27^{kip1}$, plays a crucial role in the entry of mammalian SCs into the G0 phase (Chen and Segil, 1999; Löwenheim et al., 1999). CKIs function by binding to and inhibiting the activity of the cyclin-dependent kinases that promote cell cycle progression and fulfill the cell cycle checkpoint functions (Sherr and Roberts, 1999). The $p27^{kip1}$ acts as a negative regulator of the G1-S transition in the cell cycle (Harper, 2001). Studies on $p27^{kip1}$-deficient mice have shown that when deleted, it results in the continued proliferation of SCs in postnatal mouse cochlear epithelia (Chen and Segil, 1999; Löwenheim et al., 1999). Recently, White et al. (2006) have reported that after dissociation, some of the mammalian SCs are able to recover their proliferative abilities. In addition, these dissociated SCs can also trans-differentiate into hair cells *in vitro*. These findings suggest that while these mammalian SCs might have a regenerative potential similar to avian auditory epithelia, this potential is suppressed within the tissue. This previous study also found that there was a correlation between the reduced expression levels of $p27^{kip1}$ and the ability of the mammalian supporting cells to reenter the cell cycle *in vitro*. Overall, these previous results suggest that manipulation of the $p27^{kip1}$ levels could be used therapeutically to stimulate the proliferation of mammalian SCs in tissue.

Discovery of gene inactivation by RNA interference (RNAi) has led to the development of a new targeted therapy for inner ear disease at the molecular level (Fire et al., 1998). RNAi is a two-stage intracellular process that converts the double-stranded RNA molecule precursors into functional small interfering RNAs. These small interfering RNAs are then incorporated into RNA-inducing silencing complexes. Subsequently, these duplexes unwind, with one strand used to target sequence-specific cleavage of the messenger RNAs that ultimately cause the knockdown of the expression of the targeted proteins (Elbashir et al., 2001).

* Corresponding author. Fax: +81 75 751 7225.
E-mail address: tnakagawa@ent.kuhp.kyoto-u.ac.jp (T. Nakagawa).

1044-7431/$ – see front matter © 2009 Elsevier Inc. All rights reserved.
doi:10.1016/j.mcn.2009.08.011

Although studies on $p27^{kip1}$-deficient mice have shown that its deletion results in continued SC proliferation in postnatal mouse cochlear epithelia (Chen and Segil, 1999; Löwenheim et al., 1999), the consequences of acute removal of $p27^{kip1}$ from differentiated SCs have yet to be examined. Therefore, the aim of the current study was to examine the efficacy of RNAi in silencing $p27^{kip1}$ in cochlear explant cultures from post-natal mice, and its potential for inducing mitosis in post-mitotic SCs in the cochlear epithelia after birth.

Results and discussion

Co-transfection efficiency

In this study, the two different plasmids were simultaneously introduced into the cochlear explants in order to label cells in which short hairpin RNAs (shRNAs) were transfected. To examine the efficiency of co-transfection, we introduced two different plasmids, EGFP- and DsRed-expressing vectors, into five cochlear explants via electroporation. One day after the electroporation, EGFP+ cells were found in all explants, with the majority co-expressing DsRed (Fig. 1a, b). Immunostaining for $p27^{kip1}$ identified SCs within the cochlear epithelia (Fig. 1c). DsRed was expressed in $32.5 \pm 11.0/33.0 \pm 10.9$ EGFP+, $p27^{kip1}$+ cells (98.5%), and there were $32.5 \pm 11.0/33.5 \pm 12.4$ DsRed+, $p27^{kip1}$+ cells (97.0%) that expressed EGFP. These results demonstrated that electroporation was able to simultaneously introduce two different plasmids into the SCs.

Silencing $p27^{kip1}$ expression in SCs by RNAi

ShRNA for $p27^{kip1}$-expressing vectors, sh-p27a, or the control scrambled shRNA vector, sh-scr, were co-electroporated with pEGFP-N1 into cochlear explants ($n = 5$ in each condition). Two days after the introduction of a mixture of sh-scr and pEGFPN-1, 48.4 ± 13.7 EGFP-expressing cells were found in the *whole single* cochlear explant, with all the EGFP-expressing cells positive for $p27^{kip1}$ (Fig. 2g–h'). These results indicate that transfection of plasmids into SCs did occur and that there was no silencing of the expression of $p27^{kip1}$. In sh-p27a-transfected explants, $28.4 \pm 7.8/29.7 \pm 7.7$ EGFP-expressing cells (95.4%) exhibited no expression of $p27^{kip1}$ (Fig. 2i–l), indicating that silencing of the expression of $p27^{kip1}$ occurred in these SCs.

To confirm that EGFP+ and $p27^{kip1}$-cells were SCs after the knockdown of $p27^{kip1}$, we performed immunostaining for myosin VIIa and Sox2 in explants in which sh-p27a has been introduced. Cochlear specimens of post-natal day 3 (P3) mice 1 day *in vitro* were used as the immunohistochemistry controls. In controls, immunostaining for myosin VIIa and $p27^{kip1}$ clearly demonstrated the location of the hair cells (Fig. 2a, d), and the $p27^{kip1}$–labeled SC layer (Fig. 2b, e), which was located underneath the hair cell layer. Sox2 was strongly expressed in the SCs in the organ of Corti and in the inner sulcus region (which corresponds to the interior of the organ of Corti), but in the outer sulcus region (which corresponds to the exterior of the organ of Corti), it was either faintly seen or not found at all within the SCs (Fig. 2c, f), which is identical to previous findings (Oesterle et al., 2008; Hume et al., 2007). In sh-p27a-transfected specimens ($n = 5$), double labeling for myosin VIIa and $p27^{kip1}$ demonstrated that the EGFP+ and $p27^{kip1}$-cells were located underneath the myosin VIIa+ hair cell layer (Fig. 2i'), which was coincident with the location of the SCs. Double labeling for Sox2 and $p27^{kip1}$ demonstrated that all EGFP+ and $p27^{kip1}$- cells that were located in the organ of Corti (41 cells in four explants) were positive for Sox2 (Fig. 2k-m). Overall, these results demonstrated that the introduction of sh-p27 efficiently silenced $p27^{kip1}$ expression in the SCs.

In addition, to examine the efficacy of transfection in pillar cells and Deiters' cells, immunostaining for Prox1 was performed (Kirjavainen et al., 2008). In P3 mouse cochleae, the expression of Prox1 was found in pillar cells and Deiters' cells (Fig. 3a). In sh-p27a-transfected specimens ($n = 7$), a few EGFP+ Prox1+ cells were found (Fig. 3b–d). The mean was 2.1 ± 1.9 cells in the whole single cochlea, which is $4.4 \pm 3.5\%$ of total EGFP+ cells in the whole single cochlea. Other EGFP-expressing cells were located in the outer sulcus region. In the inner sulcus region, no EGFP-expressing cells were found.

S-phase reentry of SCs by silencing $p27^{kip1}$

To examine whether $p27^{kip1}$ silencing had an effect on the reentry of SCs into the cell cycle, a 5-bromo-2-deoxyuridine (BrdU)-labeling assay was employed. To confirm that the S-phase reentry of the SCs is specific to the knockdown of $p27^{kip1}$, we used two different shRNAs to target $p27^{kip1}$ in this experiment. Explants after introduction of the plasmid mixtures, pEGFP-N1 and, sh-p27a ($n = 9$), sh-p27b ($n = 5$) or sh-scr ($n = 5$) were used. Three days after the introduction of a mixture of sh-scr and pEGFPN-1, there were no double-positive BrdU+ EGFP+ cells seen in the cochlear epithelia (Fig. 4a–d). While we found that a few mesenchymal cells located under the basement membrane of the cochlear epithelium were positive for BrdU, all of these were found to be negative for EGFP (Fig. 4a'–d'). In an explant transfected with sh-p27a, $13.8 \pm 6.8/48.2 \pm 15.2$ EGFP+ cells (28.6%) were labeled by BrdU with no expression of $p27^{kip1}$ (Fig. 4e–h'). In cochlear explants transfected with sh-p27b, BrdU+, EGFP+ cells were also found in the cochlear epithelia (Fig. 4i-l'). BrdU incorporation was identified in $7.6 \pm 4.7/24.6 \pm 15.0$ EGFP+ cells (30.9%). These results demonstrated that silencing $p27^{kip1}$ expression occurred after transfection of shRNA that was directed against *$p27^{kip1}$* and led to the initiation of S-phase reentry of the post-mitotic SCs. However, the knockdown of $p27^{kip1}$ did not induce S-phase reentry in approximately 70% of transfected cells. There are two possible

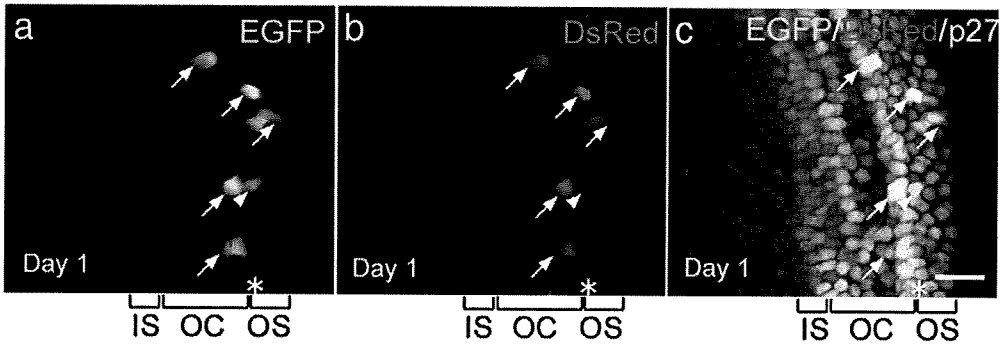

Fig. 1. Electroporation-mediated co-transfection of two different plasmids into cochlear supporting cells. Co-expression of EGFP (a) and DsRed (b) are found in supporting cells, which is identified by $p27^{kip1}$ immunostaining (c) 1 day after electroporation (arrows). An arrowhead indicates an EGFP+, DsRed- cell, and an asterisk shows an EGFP-, DsRed+ cell. IS, inner sulcus; OC, organ of Corti; OS, outer sulcus. Scale bar = 30 μm.

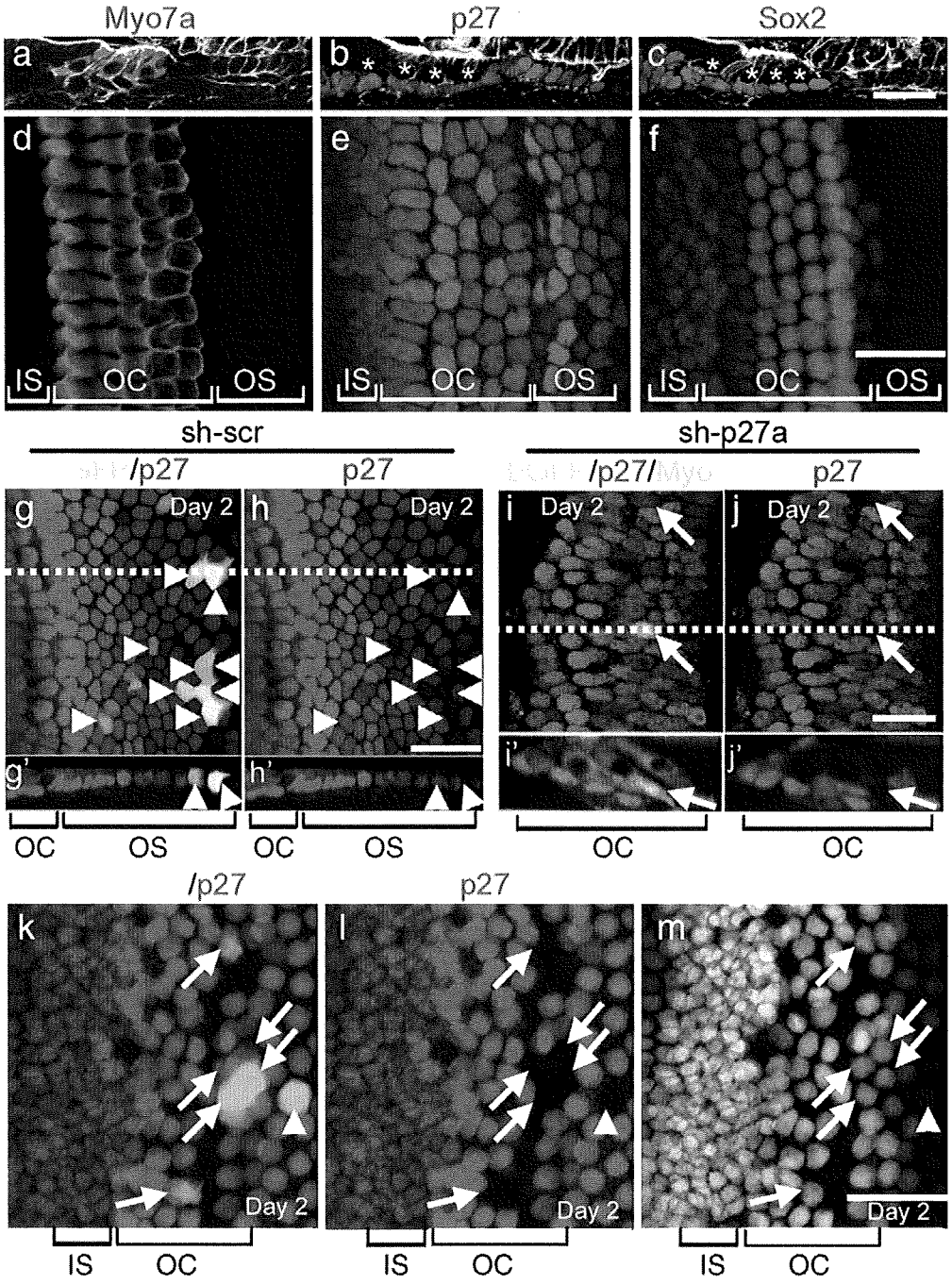

Fig. 2. Knockdown of $p27^{kip1}$ expression by RNAi occurred in supporting cells. Expression of myosin VIIa, $p27^{kip1}$ and Sox2 in sections (a–c) or in whole-mounts (d–f) are shown. Green fluorescence in a-c shows phalloidin staining. Asterisks in b, c indicate the location of hair cells. In cochlear epithelia transfected with sh-scr (g, h), EGFP+ cells (arrowheads) express $p27^{kip1}$. Cross-section images along with white dotted lines in g–j show in g'–j'. In cochlear epithelia transfected with sh-p27a (i–m), EGFP+ cells (arrows) are negative for $p27^{kip1}$. Double-labeling for myosin VIIa and $p27^{kip1}$ demonstrates the location of a transfected cell (arrow in l') corresponding to the supporting cell. Double-labeling for Sox2 and $p27^{kip1}$ (k–m) demonstrates the expression of Sox2 in EGFP+, $p27^{kip1}$- cells (arrows), indicating that $p27^{kip1}$ silencing occurs in supporting cells. A part of EGFP+, $p27^{kip1}$- cells lacks Sox2 expression (arrowhead in k–m). Myo7a, Myosin VIIa; IS, inner sulcus; OC, organ of Corti; OS, outer sulcus. Scale bars = 30 μm.

explanations for this. One is that insufficient suppression of $p27^{kip1}$, which was not enough for S-phase reentry, occurred in 70% of transfected cells. Another is that other cell-cycle inhibitors compensate the function of $p27^{kip1}$.

Mitosis in SCs induced by RNAi with $p27^{kip1}$

We performed time-lapse observations and propidium iodide (PI) staining in order to document the characteristic morphology for mitosis in SCs in which the $p27^{kip1}$ had been silenced. Two days after the introduction of a mixture of sh-p27a and pEGFPN-1, time-lapse observations of EGFP+ cells demonstrated mitosis in SCs within the explants (Fig. 5a, b, S1). We observed 10 EGFP+ cells in the outer sulcus region. In five out of the 10 EGFP+ cells that were recorded, the cells became rounded in shape and then divided into two daughter cells, which stained for BrdU but did not show any labeling for $p27^{kip1}$ (Fig. 5c, d). In addition, cross sections clearly showed nuclear migration to the luminal portion of the SCs (Fig. 5c', d'). During this process, PI staining of the nuclear chromatin demonstrated that there was segregation of the chromosomes in

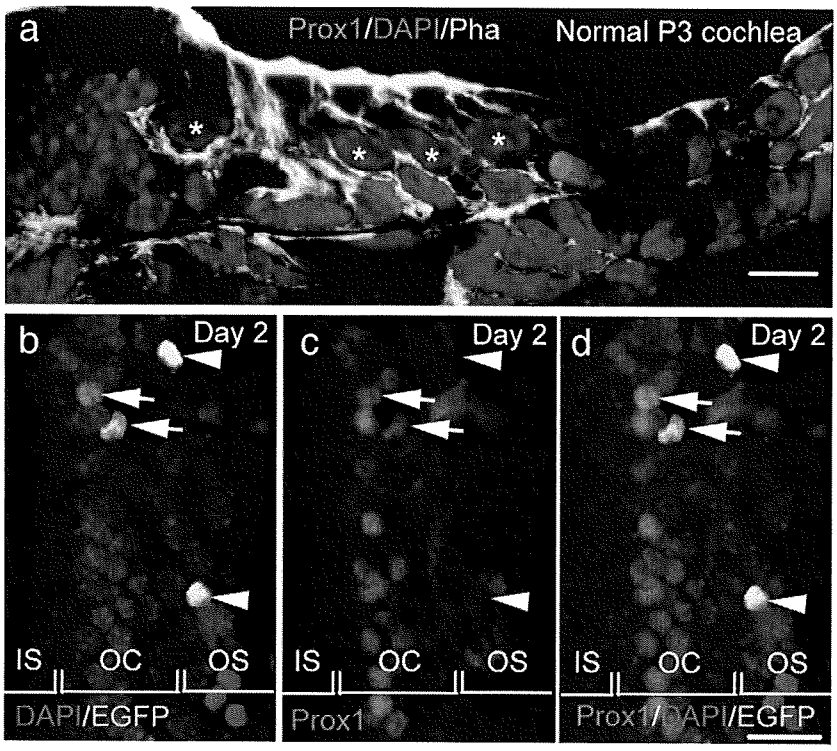

Fig. 3. Transfection in Prox1-positive supporting cells. In normal P3 cochlear epithelia, Prox1 expression (red) is seen in pillar cells and Deiters' cells (a). Green fluorescence in a shows phalloidin staining (Pha), and blue shows nuclear staining with DAPI. Asterisks in a indicate the location of hair cells. Some EGFP+ cells exhibit Prox1 expression (arrows in b–d), while other EGFP+ cells in the outer sulcus are negative for Prox1 (arrowheads in b–d). IS, inner sulcus; OC, organ of Corti; OS, outer sulcus. Scale bars = 20 μm.

the EGFP+ cells (Fig. 5e, f). Thus, these results showed that silencing of the $p27^{kip1}$ expression in post-mitotic SCs induced mitosis of the SCs in postnatal cochlear epithelia. This provides direct evidence that $p27^{kip1}$ plays a central role in controlling the proliferation of the SCs in neonatal cochleae. White et al. (2006) have reported that the capacity of SCs for proliferation is diminished depending on ages. Therefore, further experiments are required to date the efficacy of RNAi for $p27^{kip1}$ for induction of SC proliferation in adult mouse cochleae.

Fate of SCs after $p27^{kip1}$ silencing

To examine the effect of silencing $p27^{kip1}$ expression on the survival of post-mitotic SCs, we counted the number of EGFP+ cells in the cochlear epithelia that had been introduced in a mixture of pEGFPN-1 and sh-p27a or sh-scr (Fig. 6). Quantitative analysis of the EGFP+ cell survival demonstrated no significant differences in the number of surviving cells among culture periods in explants transfected with sh-scr, while there were significant reduction in the number of transfected cells was found in explants transfected with sh-p27a (Fig. 6). The number of EGFP+ cells on day 5 or 7 was significantly lower than that on day 1 or 2. These findings indicate that introduction of sh-p27a induced the loss of transfected SCs. We also examined the numbers of EGFP+, BrdU+ cells, cell-cycle reentering cells, in explants transfected with a mixture of sh-p27a and pEGFPN-1. BrdU incorporation was not found in EGFP+ cells on day 1, while on days 2-7, EGFP+, BrdU+ cells were observed in explants that had been introduced sh-p27a. There were significant differences in the number of EGFP+, BrdU+ cells between day 2 and day 3, 5, or 7 (Fig. 6). Fig. 6 indicates that the reduction of EGFP+ cells between day 2 and 3 mainly caused by the reduction of EGFP+, BrdU+ cells, and that the reduction of EGFP+ cells between day 3 and 5 was due to the loss of EGFP+, BrdU- cells. Therefore, both reentry of cell cycle by silencing $p27^{kip1}$ expression and silencing $p27^{kip1}$ expression itself may induce degeneration of transfected SCs.

We then investigated the cell death mode that occurred after silencing $p27^{kip1}$ expression. Immunohistochemical labeling for cleaved caspase 3 along with PI staining was performed in the explants 3 days after introduction of a mixture of sh-p27a and pEGFPN-1. The activation of caspase 3 was identified in 9/327 EGFP+ cells in six explants (Fig. 7a). PI staining showed the fragmentation of nuclear chromatin in EGFP+ and cleaved caspase 3+ cells (Fig. 7b). In addition, we examined the effects of the addition of a caspase 3 inhibitor to the culture medium. Addition of the caspase 3 inhibitor significantly increased the number of EGFP+ cells in explants transfected with sh-p27a (two-way factorial ANOVA, $p<0.0001$, Fig. 8). However, the caspase 3 inhibitor did not completely prevent the loss of EGFP+ cells, as over time, the explants treated with the caspase 3 inhibitor exhibited a decrease in their numbers (Fig. 8). All these results indicated that silencing the $p27^{kip1}$ expression in post-mitotic SCs initiated apoptosis in at least some, but not all of the cells. These results are consistent with previous data reported for apoptosis in mouse hair cells after the deletion of pRb (Mantela et al., 2005; Sage et al., 2005; Weber et al., 2008), $p19^{ink4d}$ (Chen et al., 2003) or both $p19^{ink4d}$ and $p21^{cip1}$ (Laine et al., 2007). On the other hand, the results indicate that other mechanisms rather than degradation via apoptosis are involved in the loss of transfected SCs. Hence, further investigations are necessary to reveal mechanisms for the loss of transfected SCs.

On the other hand, even at 7 days after the introduction of a mixture of sh-p27a and pEGFPN-1, EGFP+, BrdU+ cells were still observed in cochlear epithelia that had been transfected with sh-p27a. To examine the potential of silencing $p27^{kip1}$ expression for trans-differentiation of SCs into hair cells, specimens that had been transfected with sh-p27a were immunohistochemically labeled for myosin VIIa. The results showed that there was no myosin VIIa

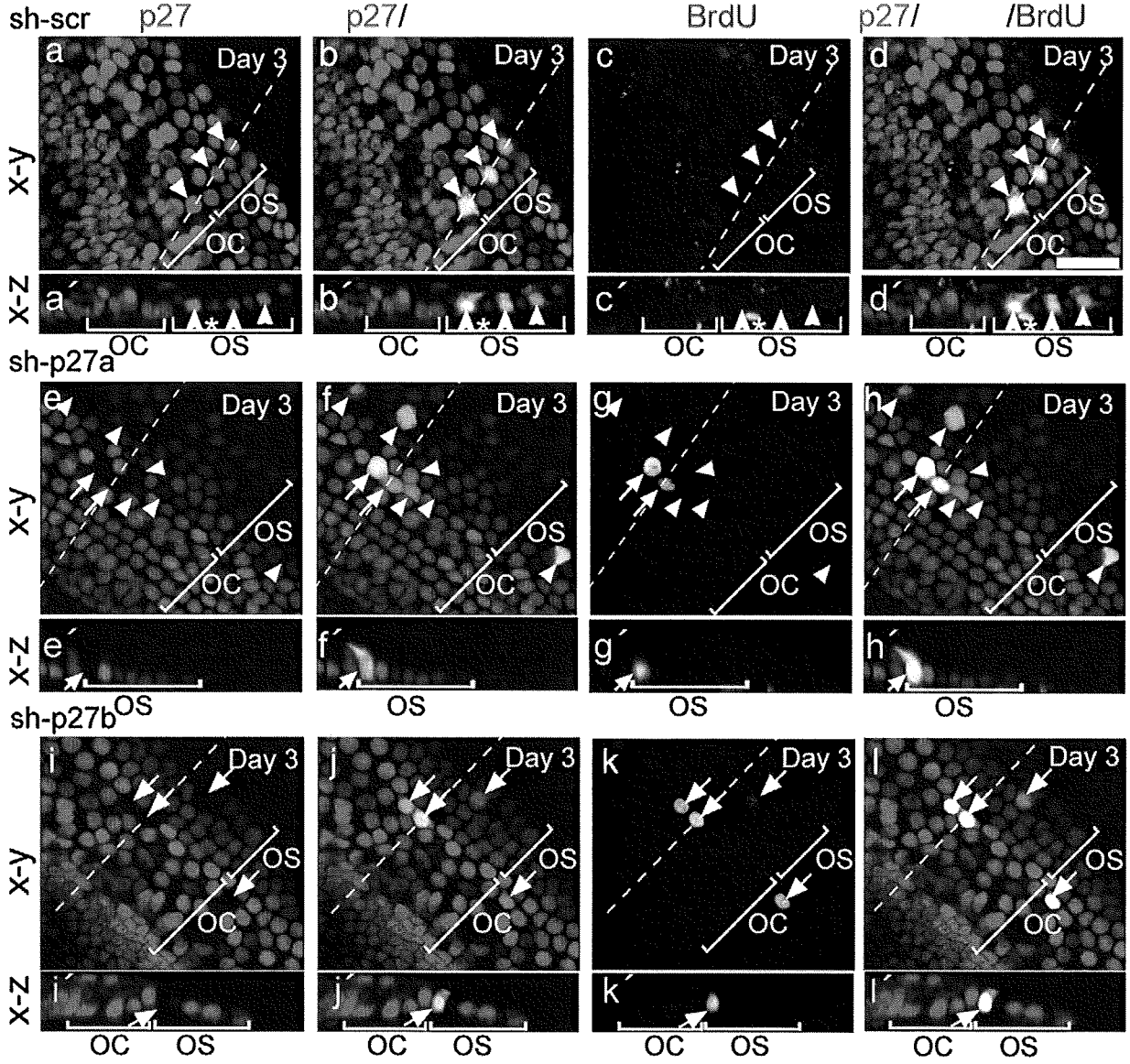

Fig. 4. Supporting cells silenced $p27^{kip1}$ by RNAi reenter S-phase. In cochlear epithelia following introduction of sh-scr, EGFP+ cells exhibit expression of $p27^{kip1}$ and are negative for BrdU (arrowheads in a–d). In cross-section images (a'–d') along with white dotted lines in a–d, a cell located underneath the cochlear epithelium shows BrdU incorporation (asterisk). In cochlear epithelia following introduction of sh-p27a (e–h) or sh-p27b (i–l), some of EGFP+, $p27^{kip1}$- cells exhibit BrdU incorporation (arrows). Other EGFP-positive cells (arrowheads in e–h) show silencing of $p27^{kip1}$, but no incorporation of BrdU. OC, organ of Corti; OS, outer sulcus. Scale bar = 30 μm.

labeling noted in the EGFP+ cells on days 5 and 7 (data not shown). These findings indicate that no SCs in which the $p27^{kip1}$ expression had been silenced underwent the trans-differentiation into hair cells. On the other hand, a separate study that used dissociated SCs showed the ability of post-mitotic SCs to trans-differentiate into hair cells in combination with the downregulation of $p27^{kip1}$ *in vitro* (White et al., 2006). Therefore, it appears that further manipulations are required in order to achieve hair cell regeneration in tissue.

When there is manipulation of Notch signaling by gene transfer (Kawamoto et al., 2003) or by pharmacological inhibitors (Yamamoto et al., 2006), the formation of ectopic hair cells in the outer sulcus region was observed, suggesting that SCs in this region are able to retain their ability to trans-differentiate into hair cells. In the avian auditory epithelium, the loss of hair cells is a key trigger that leads to the conversion of SCs to hair cells, a process for which Notch signaling is also involved (Stone and Rubel, 1999; Cafaro et al., 2007). In the mammalian cochlear epithelium, transient activation of Notch signaling has been observed in SCs following hair cell loss (Hori et al., 2007; Batts et al., 2009), suggesting that additional manipulation of Notch signaling in SCs could possibly contribute to the regeneration of hair cells once there is induction of SC proliferation by RNAi with $p27^{kip1}$.

Sage et al. (2005) demonstrated that there was proliferation of SCs in the cochlear epithelia of pRb−/− mice, indicating that pRb can be a target to induce cell-cycle reentry of post-mitotic SCs in tissue. However, pRb expression is undetectable in SCs in post-natal cochlear epithelia in normal mice (Mantela et al., 2005). Therefore, pRb expression does not appear to be an attractive candidate for induction of mitosis in post-natal SCs. In contrast, post-natally in normal mice, the $p27^{kip1}$ expression is strong and stable in the SCs (Chen and Segil, 1999; Löwenheim et al., 1999; Endo et al., 2002; White et al., 2006). Based on these reports, we considered $p27^{kip1}$ to be an appropriate target for induction of SC proliferation in the mammalian cochlear epithelium.

In conclusion, this is the first report showing induction of mitosis in post-mitotic mammalian SCs in tissue by RNAi targeting of $p27^{kip1}$. The present findings indicate that $p27^{kip1}$ expression is sufficient for

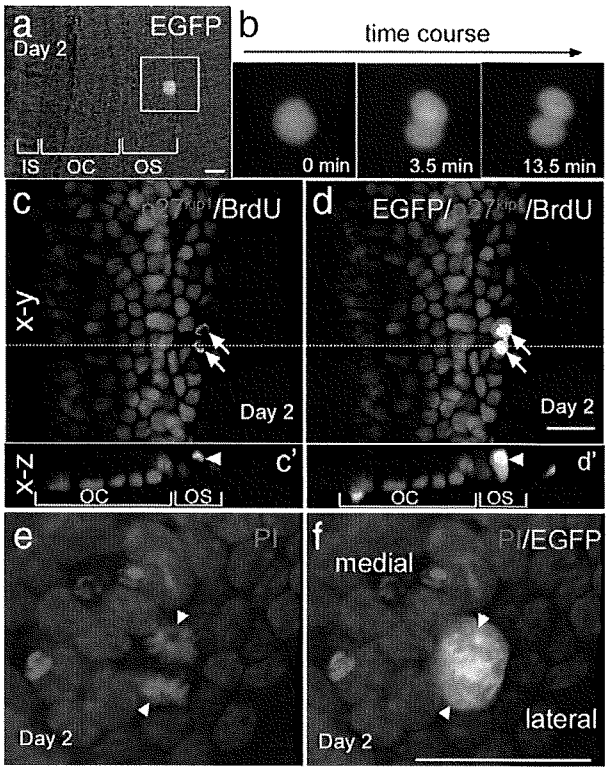

Fig. 5. Mitosis in supporting cells silenced $p27^{kip1}$ by RNAi. Time-lapse observation demonstrates division of sh-p27a-transfected supporting cells (a, b). A dividing cell expressing EGFP is positive for BrdU, but not for $p27^{kip1}$ (arrows in c, d). Cross-section images along with white dotted lines in c, d show migration of a BrdU+ nucleus to the luminal surface of the supporting cell (arrowheads in c', d'). An EGFP+ supporting cell in the outer sulcus region exhibits the segregation of chromosomes (arrowheads in e, f). PI, Propidium iodide, IS, inner sulcus; OC, organ of Corti; OS, outer sulcus. Scale bars = 30 μm.

maintaining the post-mitotic state of the SCs in tissue, and that RNAi is an efficient strategy for knockdown of the expression of $p27^{kip1}$ in the SCs of post-natal mammalian cochlear epithelia. On the other hand, our data have also identified obstacles that need to be overcome in order to achieve hair cell regeneration via the stimulation of SC proliferation. The most critical of these factors is the activation of the apoptotic pathways in SCs after silencing the expression of $p27^{kip1}$. Induction of trans-differentiation of the SCs into hair cells is also indicated obstacles to be overcome. Therefore, further manipulations

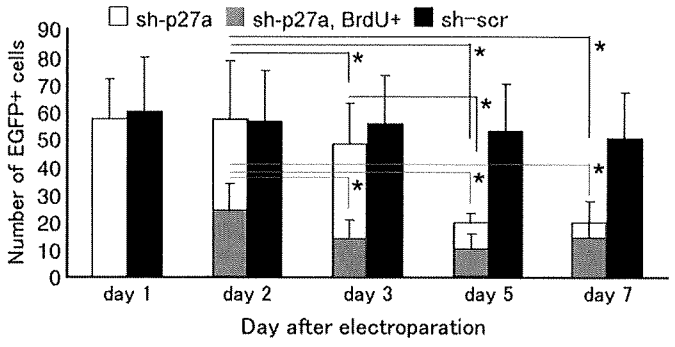

Fig. 6. Effects of silencing $p27^{kip1}$and cell-cycle reentry on transfected supporting cell survival. The surviving EGFP+ cell numbers in sh-scr-transfected explants (black column) show no significant alteration among culture periods, while those in sh-p27a-transfected explants (white column) significantly decreased over time. Significant decreases in numbers EGFP+, BrdU+ cells that have reentered cell-cycle, in sh-p27a-transfected explants (grey column)are observed on days 3–7 in comparison with day 2. Asterisks indicate statistical significance with the Tukey–Kramer test. Bars represent standard deviation.

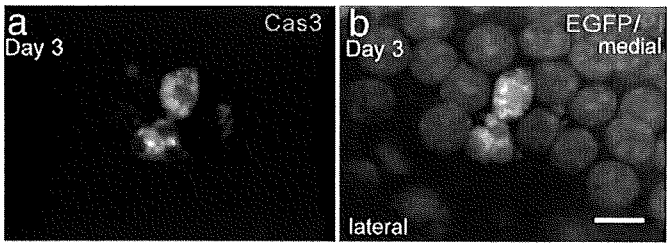

Fig. 7. Activation of caspase 3 in supporting cells that had been silenced $p27^{kip1}$ in the outer sulcus region. The expression of cleaved caspase 3 is found in sh-p27a-transfected supporting cells (a). PI staining exhibits the fragmentation of nuclear chromatins in sh-p27a-transfected supporting cells expressing EGFP (b). Scale bar = 10 μm.

are required for preventing apoptosis and induction of trans-differentiation into hair cells to achieve hair cell regeneration by downregulating $p27^{kip1}$.

Experimental methods

Animals

ICR mice (Japan SLC Inc., Hamamatsu, Japan) were maintained at the Institute of Laboratory Animals, Graduate School of Medicine, Kyoto University, Japan. Experimental protocols were approved by the Animal Research Committee of Kyoto University Graduate School of Medicine (MedKyo07062), and complied with the US National Institutes of Health (NIH) Guidelines for the Care and Use of Laboratory Animals.

Explant culture

P3 ICR mice were deeply anesthetized with carbon dioxide and decapitated. The temporal bones were dissected out and the cochleae removed from the surrounding tissue in 0.01 M phosphate-buffered saline (PBS), pH 7.4, which was supplemented with 0.2% glucose. The lateral walls were removed from the cochleae and the cochlear epithelia were dissected from the cochlear modiolus and placed intact on sterile membranes in culture inserts (12 mm Millicell CM, Millipore, Billerica, MA). These explants were maintained in 24-well culture plates (Iwaki, Tokyo, Japan) in minimum essential medium (MEM; Invitrogen, Carlsbad, CA) supplemented with 3 mg/ml glucose and 0.3 mg/ml penicillin G potassium salt (Nacalai Tesque, Kyoto, Japan), at 37 °C in a humidified atmosphere of 95% air and 5% CO_2 for 24 h. The cultured explants were then used for the electroporation experiments.

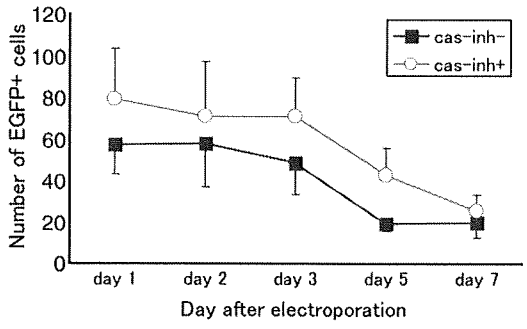

Fig. 8. Effect of a caspase 3 inhibitor on the number of surviving supporting cells following $p27^{kip1}$silencing. Closed squares show the numbers of EGFP+ cells in sh-p27a-transfected explants cultured without a caspase 3 inhibitor, and open circles show those with a caspase 3 inhibitor. An overall effect of application of a caspase 3 inhibitor is significant at $p<0.001$ with two-way factorial ANOVA, no significant differences in the numbers of EGFP+ cells were identified with pair-wise comparisons with Tukey–Kramer test. Bars represent standard deviation.

Plasmids

ShRNAs are RNA sequences that make tight hairpin turns and can silence gene expression via RNAi (Paddison et al., 2002). These sequences are expressed in vectors and can be used to target the *p27^{kip1}* coding sequence (sh-p27) or to act as a control scrambled sequence (sh-scr). The two different sh-p27s prepared for this experiment were sh-p27a and sh-p27b. The sequences were 5′-AGACAATCAGGCTGGGTTA-3′ for sh-p27a, 5′-GAAGCGACCTGCTGCA-GAA-3′ for sh-p27b and 5′-TACGCGCATAAGATTAGGG-3′ for the sh-scr control sequence. These complementary sequences were inserted into the mU6 pro vector. The efficacy of sh-p27s in silencing the p27^{kip1} expression in neuronal cells has been previously demonstrated (Kawauchi et al., 2006). pEGFP-N1 and pDsRed-Express-N1 vectors were purchased from Clontech (Palo Alto, CA). Each plasmid DNA was propagated in DH5α *Escherichia coli* and purified using an Endo Free Plasmid Maxi Kit (Qiagen, Valencia, CA). The yield and purity of the plasmid DNA was evaluated using an Ultrospec 3300pro spectrophotometer (GE Healthcare, Tokyo, Japan).

Electroporation

For the electroporation experiments, we prepared four kinds of plasmid mixtures that included, pDsRed-Express-N1 and pEGFP-N1, sh-p27a and pEGFP-N1, sh-p27b and pEGFP-N1 and sh-scr and pEGFP-N1. All vectors were diluted in electroporation buffer (125 mM NaCl, 5 mM KCl, 1.5 mM $MgCl_2$, 10 mM glucose, 20 mM HEPES, pH 7.4) to a concentration of 1.5 mg/ml. A CUY21 electroporator (Nepa Gene, Chiba, Japan) was used to transfer the plasmid mixtures into the auditory epithelial cells from the explant cultures. Culture inserts were placed on the lower platinum electrode, with 10 μl of the plasmid DNA solution then applied between them. Eight rectangular pulses (14 V, 50 ms duration at 100-ms intervals) were passed from the upper to the lower electrodes, followed by an additional eight pulses that were applied from the lower to the upper electrodes. Afterwards, explant cultures were maintained in culture medium supplemented with 3 μg/ml BrdU (Sigma-Aldrich, St. Louis, MO) for 1–7 days. The culture medium was changed daily. Ten cochlear epithelia were used for a single culture, with ten independent cultures performed.

Immunohistochemistry

Explants were fixed in 4% paraformaldehyde (PFA) in PBS for 15 min at room temperature, washed with 0.2% Triton-X 100 in PBS (Triton-PBS) and stained as whole mounts. After blocking with 10% normal goat serum in Triton-PBS at 4 °C for 60 min, the explants were incubated overnight with the following primary antibodies: anti-mouse p27^{kip1} rabbit polyclonal antibody (1:500; Lab Vision, Fremont, CA), anti-myosin VIIa rabbit polyclonal antibody (1:500; Proteus Bioscience, Ramona, CA), anti-Sox2 goat polyclonal antibody (1:500, Santa Cruz Biotechnology, Inc., Santa Cruz, CA), anti-Prox1 rabbit polyclonal antibody (1:1000; Chemicon, Temecula CA), anti-BrdU mouse monoclonal antibody (1:100; Becton Dickinson, Franklin Lakes, NJ), and anti-cleaved caspase-3 mouse monoclonal antibody (1:100; #9661S, Cell Signaling Technology, Danvers, MA). Alexa Fluor 594-conjugated anti-rabbit antibody, Alexa Fluor 633-conjugated anti-mouse, or anti-rabbit antibody (1:500; Invitrogen) was used as the secondary antibody and Vectashield (Vector Laboratories, Burlingame, CA) was used for mounting the samples. For BrdU staining, the specimens were pre-treated in 2N HCl for 20 min at 37 °C, and neutralized with 0.01M PBS (pH 8.5) for 10 min at room temperature. To label for both myosin VIIa and p27^{Kip1} simultaneously, a Zenon™ Alexa Fluor 647 Rabbit IgG Labeling Kit (Invitrogen) was used. PI (Invitrogen) was used to stain nuclear chromatin. Images were acquired using a confocal laser scanning system (TCS SP2, Leica Microsystems, Wetzlar, Germany).

Co-transfection efficiency

To examine the efficiency of co-transfecting two different plasmids, we used five explants that were transfected with a mixture of pEGFPN-1 and pDsRed-Express-N1 vectors. To identify the location of the SCs in the cochlear epithelia, the explants were labeled immunohistochemically for p27^{kip1} 1 day after the electroporation. We then quantified the number of p27^{kip1}+ cells that were also EGFP+ and/or DsRed+.

Silencing p27^{kip1} expression in SCs by RNAi

To examine the efficiency of silencing p27^{kip1} in sh-p27-transfected SCs, explants were transfected with a mixture of sh-scr and pEGFPN-1, sh-p27a and pEGFPN-1 or sh-p27b and pEGFPN-1 2 days prior to being immunolabeled for p27^{kip1} ($n=5$ in each condition). We then quantified the number of p27^{kip1}-EGFP+ and EGFP+ cells in the cochlear epithelia. To examine the location of EGFP+ cells in the cochlear epithelium, we counted the number of EGFP+ cells in the outer sulcus region, in the organ of Corti and in the inner sulcus region in sh-p27a-transfected specimens.

To confirm that EGFP+ and p27^{kip1}-cells were SCs after the knockdown of p27^{kip1}, immunohistochemistry for p27^{kip1} and myosin VIIa or Sox2 was performed in explants 2 days after sh-p27a introduction ($n=5$ for myosin VIIa, $n=4$ for Sox2). To examine the efficacy of transfection in pillar cells and Deiters' cells, immunostaining for Prox1 was performed in explants 2 days after sh-p27a introduction ($n=7$). In order to demonstrate normal distributions of these molecules, we used frozen sections or whole mounts of P3 ICR mouse cochleae after 1 day *in vitro* ($n=10$) for the immunohistochemistry controls. At the end of the staining procedures, we used FITC-phalloidin (Invitrogen) to counterstain the specimens.

S-phase reentry of SCs by silencing p27^{kip1}

To examine the effect of silencing p27^{kip1} expression on the S-phase reentry of SCs, we used cochlear explants that were introduced a mixture of sh-p27a ($n=9$), sh-p27b ($n=5$) or sh-scr ($n=5$) and pEGFPN-1 3 days prior to labeling the explants for p27^{kip1} and BrdU. We then counted the number of BrdU+ EGFP+ cells and EGFP+ cells for each group.

Mitosis in SCs induced by RNAi with p27^{kip1}

To examine the effect of p27^{kip1} silencing on SC division, we used cochlear explants that were introduced a mixture of sh-p27a and pEGFPN-1 ($n=10$) 2 days prior to making time-lapse recordings of the explants using the BZ-9000 system (Keyence, Osaka, Japan). In the different explants, still images were captured for 10 EGFP-expressing cells. Immediately after the time-lapse observations were recorded, the specimens were fixed with 4% PFA for 15 min at room temperature, and then stained immunohistochemically for p27^{kip1} and BrdU or with PI.

Fate of SCs after p27^{kip1}silencing

To determine the effect of p27^{kip1} silencing on the survival and differentiation of post-mitotic SCs, mixtures of sh-p27 and pEGFPN-1 or sh-scr and pEGFPN-1 were introduced into cochlear explants at 1, 2, 3, 5 and 7 days ($n=5$–10) prior to the counting of the number of EGFP+ or EGFP+, BrdU+ cells.

Six explants into which a mixture of sh-p27a and pEGFPN-1 had been introduced 3 days earlier were labeled immunohistochemically for cleaved caspase 3 and stained with PI in order to investigate the